CALIFORNIA INSTITUTE OF TECHNOLOGY

EARTHQUAKE ENGINEERING RESEARCH LABORATORY

A PERFORMANCE-BASED OPTIMAL STRUCTURAL DESIGN METHODOLOGY

BY

JAMES L. BECK, COSTAS PAPADIMITRIOU,
EDUARDO CHAN AND AYHAN IRFANOGLU

REPORT NO. EERL 97-03

A REPORT ON RESEARCH SUPPORTED BY KAJIMA CORPORATION AND THE NATIONAL SCIENCE FOUNDATION

PASADENA, CALIFORNIA

1997

THIS REPORT IS BASED UPON WORK WHICH BEGAN UNDER THE CUREE-KAJIMA RESEARCH PROGRAM OF THE CALIFORNIA UNIVERSITIES FOR RESEARCH IN EARTHQUAKE ENGINEERING AND CONTINUED UNDER GRANT CMS-9706135 FROM THE NATIONAL SCIENCE FOUNDATION. THE INITIAL VERSION OF THE CODA SOFTWARE PACKAGE WAS DEVELOPED AS A TEAM EFFORT BY THE AUTHORS AND H. A. SMITH, V. VANCE AND L. BARROSO OF STANFORD UNIVERSITY AND S. F. MASRI AND W. M. XU OF THE UNIVERSITY OF SOUTHERN CALIFORNIA.

A PERFORMANCE-BASED OPTIMAL STRUCTURAL DESIGN METHODOLOGY

by

James L. Beck, Costas Papadimitriou, Eduardo Chan and Ayhan Irfanoglu

Report No. EERL 97-03

California Institute of Technology
Pasadena, California
October 1998

A PERFORMANCE-BASED OPTIMAL STRUCTURAL DESIGN METHODOLOGY

J.L. BECK, C. PAPADIMITRIOU, E. CHAN, A. IRFANOGLU
Division of Engineering and Applied Science, California Institute of Technology, Pasadena, California 91125, USA

SUMMARY

A general framework for multi-criteria optimal design is presented which is well-suited for performance-based design of structural systems operating in an uncertain dynamic environment. A decision theoretic approach is used which is based on aggregation of preference functions for the multiple, possibly conflicting, design criteria. This allows the designer to trade off these criteria in a controlled manner during the optimization. Reliability-based design criteria are used to maintain user-specified levels of structural safety by properly taking into account the uncertainties in the modeling and seismic loads that a structure may experience during its lifetime. Code-based requirements are also easily incorporated into this optimal design process. The methodology is demonstrated with two simple examples involving the design of a three-story steel-frame building for which the ground motion uncertainty is characterized by a probabilistic response spectrum which is developed from available attenuation formulas and seismic hazard models.

1 INTRODUCTION

The decision-making process in the design of civil engineering systems requires the selection of the most promising choice for the design from a large set of possible alternatives, based on an evaluation using specified criteria reflecting the acceptability of a design. Such criteria usually include costs, structural engineering criteria, client preferences, social, political, legal and economic considerations, and liabilities from uncertain risks arising, for example, from construction practice and environmental loads such as earthquakes and strong winds. In particular, in order to be able to trade off reliability of performance and structural costs in the design process, the uncertainties in the structural response due to the uncertainties in the loads exciting the structure must be considered (Ang and Cornell 1974, Wen 1995, Ang et al. 1996, Beck et al. 1996a, 1996b). These uncertainties, particularly for seismic loads, can be very influential factors in the design decisions.

Numerous studies on single- and multi-objective reliability-based optimization with applications in the design of structural systems have been published, including Moses and Kisner (1967), Frangopol (1985), Casciati and Faravelli (1985), Thoft-Christensen and Murotsu (1986), Fu and Frangopol (1990a, 1990b) and the contributions in the book edited by Adeli (1994). The purpose of such studies is to find the optimal values of a set of design parameters that minimize one or more objective functions, such as total weight, total cost, or element or system failure probabilities, subject to constraints involving design conditions such as geometric constraints and strength criteria.

Recently, a new framework for computer-aided multi-criteria optimal design has been presented which allows all the different design criteria to be traded off while accounting for modeling and loading uncertainties (Beck et al. 1996a, 1996b). A software package called CODA has been developed to implement the new multi-criteria optimal design framework using relatively new methodologies such as object-oriented programming, multi-criteria decision theory, stochastic optimization (including genetic algorithms) and reliability integral approximations (Beck et al. 1996a). The development of this computer-aided multi-criteria optimal design tool allows the designer to rapidly evaluate and improve a proposed design by taking into account the major factors of interest related to design, construction, and operation of a structure in the presence of risk.

In the present work, the methodology is shown to be well-suited to the concept of performance-based design for several reasons. First, it can simultaneously consider multiple performance level requirements while searching for an optimum structural design. Second, it can easily incorporate reliability-based design criteria. It is also demonstrated that existing reliability-based optimal design formulations can be viewed as special cases of the present approach. Moreover, the optimal solutions provided by the proposed framework belong to the multi-objective Pareto optimal set (Cohon 1978).

In the following sections, the multi-criteria optimal design framework is presented, an overview of the CODA software is given and then the methodology is demonstrated with two examples involving the design of a three-story steel-frame building in the presence of seismic risk. In both examples, the ground motion is characterized by a probabilistic response spectrum which is developed from available attenuation formulas and seismic hazard models. In the first example, optimal design results are presented for three different seismicity levels

which involve trading off reliability of performance and structural cost while meeting code-based design criteria. A comparison is made between the optimal design for a continuous range of possible member sections and for a discrete set of AISC W-shape sections (AISC 1989). In the second example, application of the methodology to the performance-based design of the three story building is presented. For demonstration purposes, the four performance levels suggested in SEAOC's *Vision 2000* (1995) are used in terms of specified interstory drift ratio limits and their corresponding reliabilities.

2 OPTIMAL DESIGN METHODOLOGY

2.1 Introduction

The design decision-making process is an iterative procedure where a preliminary design is cycled through stages of analysis, evaluation, and revision to achieve a design which is optimum in some chosen sense. In the proposed optimal design methodology, a formal treatment of these three design stages is made so that the decision-making process can be implemented in software to aid the designer in selecting an optimal design. The methodology handles the key aspects of decision-making in a design process in a consistent and rational way. Also, uncertainties related with the structural design are incorporated into the design process in a quantitative and explicit way so as to allow a formal treatment of their effects on the resulting design.

Structural design starts with an as comprehensive as possible description of the design problem. The designer must specify all design requirements, or design criteria, on which each design is to be judged, including the performance parameters involved in each design criteria. The designer then chooses a physical configuration as well as individual structural member geometrical and connection information to give a preliminary design. At this stage, the designer needs to specify all possible loading cases that the structure might experience during its lifetime. Clearly, the choice of these cases is of utmost importance since the structural design is greatly affected by the loadings considered.

In the next stage of the design process, all structural performance parameters of the structure under the chosen loading cases are computed through some chosen analysis methods. It is important to realize that whichever response analysis method is used, for example, static, quasi-dynamic (e.g. response spectrum based) or dynamic analysis methods, there will be an uncertainty in the results computed due to the uncertainties in the loads applied to the structure and due to the uncertainties related with the modeling of the structure. A rational treatment of these uncertainties and their effects on the design can be made by using probabilistic analysis tools to incorporate them into the analysis of the structural performance.

The designer must then use the calculated performance parameter values to judge how well each design criterion is satisfied. In general, each such criterion will not be optimally satisfied by the preliminary design. The designer must then revise the initial design in order to obtain a better one by trying to better satisfy all the design criteria. In general, however, it will not be possible to optimally satisfy each criterion because some of them will be conflicting.

Therefore, some compromise, or trade-off, must be performed when seeking a better design.

This process of analysis, evaluation and revision is repeated iteratively, and as long as it is necessary, to find a design which is considered to give the best compromise solution to all the design criteria. It is now shown how this structural design process can be converted into a performance-based multi-criteria optimization problem.

2.2 The Analysis Stage

For the analysis stage of the optimal design methodology, the designer must specify what the design and performance parameters of interest are. These design and performance parameters are used to express the level of satisfaction of the design criteria in a quantitative manner so that an overall design performance measure can be computed for each design.

The design parameters, designated by a vector $\boldsymbol{\theta}$, are those parameters of the design which are selected to be varied during the search for an optimal design. For example, design parameters may take the form of geometric information for the structural members, such as member cross-sectional dimensions. On the other hand, performance parameters, designated by a vector $\mathbf{q}$, represent quantities related to the "performance" of the design, and can take the form of conventional structural parameters (e.g. stress, deflection, interstory drift) or other parameters (e.g. structural reliability, material cost of the structural system). Obviously, the performance parameters, $\mathbf{q}(\boldsymbol{\theta})$, are functions of the current design parameters, $\boldsymbol{\theta}$.

Structural performance parameters under "deterministic" (code-based) loads can be computed using a finite-element model of the structure which is specified by the design parameters. The construction cost can be computed using a costing algorithm. On the other hand, reliability-based performance parameters, such as the uncertain peak lifetime interstory drift, must be analyzed using probabilistic analysis tools and a probabilistic seismic hazard model, as described later.

2.3 The Evaluation Stage

The objective of the evaluation stage of the optimal design methodology is to obtain an overall design evaluation measure $\mu(\boldsymbol{\theta})$ for the design specified by the current value of the design parameter vector $\boldsymbol{\theta}$. This measure $\mu(\boldsymbol{\theta})$ serves as an objective function which, at the revision stage, is used to determine improved, or optimal, designs.

In general, for evaluation of the design, the designer may wish to impose many different design criteria. Therefore, a multi-criteria decision methodology is required in which a design is quantitatively evaluated on the basis of each design criterion (Keeney and Raiffa 1976, Cohon 1978, French 1988). Furthermore, since not every design criterion can be satisfied to its maximum extent simultaneously with the other design criteria, the methodology must allow a trade-off to occur between conflicting criteria in the optimization process. To be able to do the trading-off in a controlled manner, the designer should be given the freedom to set the relative importance of each design criterion explicitly.

In order to perform a quantitative evaluation of the current design, a preference function μ_i, $i = 1, \ldots, N_c$, for each of the N_c design criteria is specified. Here, each μ_i defines the preference for the various values of each design parameter or performance parameter involved

in the corresponding criterion. A preference function may simply express a minimum and/or maximum fuzzy bound on a design quantity, or it may express a more complex design criterion. A larger preference value for one performance parameter value compared with another implies that the user prefers the first parameter value more than the other value. Also, to be able to formulate the preferences in a consistent way, the values that a preference function can take must lie in a standard range, taken as the unit interval $[0, 1]$. Figure 1 shows a preference function for the design criterion that the maximum interstory drift should not exceed some code prescribed value. In this case, the user prefers most the maximum interstory drift values which are less than 90% of the code-specified drift value, since the preference function has its greatest possible value there. On the other hand, the user considers values of the maximum interstory drift which exceed the code-specified drift value as unacceptable, since the preference function is zero (the least possible value) there.

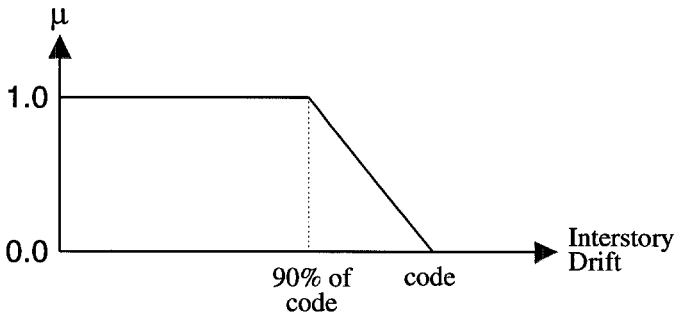

Figure 1: Preference Function for the Code-Based Interstory Drift Ratio

As shown in Figure 1, a linear fall-off has been chosen for those values of the maximum interstory drift which lie between 90% and 100% of the code-specified drift value.

Another interpretation of a preference function is that it specifies the degree of satisfaction of a design criterion for each value of the design or performance parameters involved; an extreme value $\mu_i(\mathbf{q}(\boldsymbol{\theta})) = 1$, or $\mu_i(\mathbf{q}(\boldsymbol{\theta})) = 0$, implies that the current design specified by $\boldsymbol{\theta}$ perfectly satisfies, or does not satisfy at all, respectively, the i-th design criterion. Still another interpretation is to view the preference function as a membership function for the fuzzy set of "acceptable performance" as judged by the i-th design criterion. In this case, an extreme value $\mu_i(\mathbf{q}(\boldsymbol{\theta})) = 1$, or $\mu_i(\mathbf{q}(\boldsymbol{\theta})) = 0$, implies that on the basis of the i-th design criterion, the current design specified by $\boldsymbol{\theta}$ is definitely acceptable, or definitely unacceptable, respectively. Intermediate values express the degree of performance acceptance given by the design.

Any constraints directly imposed on the design parameters, such as geometrical constraints, are treated as additional design criteria. Each such criterion is expressed as a "soft" constraint through a preference function. For example, a preference function similar to the one shown in Figure 1 can be used to express a "soft" upper bound on a design parameter. If the designer also wishes to impose a lower bound on the parameter, then a two-sided version of the preference function can be used (see Figure 11 for various preference function examples). By treating design parameter constraints in this way, the degree to which the constraint is

satisfied can be traded off against other design criteria during the optimization of the design.

In addition, to be able to combine different design criteria in a preferred manner to obtain a measure for the overall rating of the design, the designer must specify importance weights, w_i, $i = 1, \ldots, N_c$, which indicate the relative importance of each of the design criteria. Increasing the value of an importance weight for a design criterion gives it more influence in the trade-off which occurs between the various conflicting criteria during optimization of the design, that is, the new design should be such that the preference function value corresponding to that criterion should have a higher value in the optimal design.

As anticipated, the final step in the evaluation stage is to compute an overall design evaluation measure $\mu(\boldsymbol{\theta})$ on the basis of the quantitative evaluations, $\mu_i(\mathbf{q}(\boldsymbol{\theta}))$, $i = 1, \ldots, N_c$, of the design for each of the N_c design criteria. This is done by a preference aggregation rule which must satisfy certain consistency requirements. In general, different aggregation rules give different design strategies for trading off the design criteria, and so lead to different optimal designs.

A preference aggregation rule is simply a functional relationship, f, between the overall design evaluation measure, μ, and the individual preference values, $\mu_1, \mu_2, \ldots, \mu_{N_c}$, for all of the design criteria (Keeney and Raiffa 1976). An optimal design for a given preference aggregation rule is therefore given by a design parameter vector $\boldsymbol{\theta}$ which maximizes:

$$\mu(\boldsymbol{\theta}) = f(\mu_1(\mathbf{q}(\boldsymbol{\theta})),\ \mu_2(\mathbf{q}(\boldsymbol{\theta})),\ \ldots,\ \mu_{N_c}(\mathbf{q}(\boldsymbol{\theta}))) \tag{1}$$

where it is understood that some of the preference functions μ_i may correspond to design parameter constraints and, therefore, depend directly on the design parameter values.

Axioms of consistency imposed on the preference aggregation rule are (Otto 1992):

1. The overall design evaluation measure μ lies in the unit interval $[0, 1]$, with $\mu = 1$ for a perfectly acceptable design and $\mu = 0$ for a completely unacceptable design.

2. μ is a monotonically increasing continuous function of each μ_i. The monotonicity ensures that if the design is changed to give higher preference for the i-th design criterion while the preference values for the other design criteria remain unchanged, the overall preference for the design must increase (or possibly remain unchanged). Also, continuity ensures that a small change in the preference for a design based on any of the design criteria produces only a corresponding small change in μ.

3. $\mu_0 = f(\mu_0, \mu_0, \ldots, \mu_0)$, that is, if the individual preferences for a design based on each criterion have the same value, then the overall preference for the design must have this value.

4. $\mu = 0$ if and only if $\mu_i = 0$ for some i, that is, a design is completely unacceptable in the overall sense if and only if it is completely unacceptable on the basis of at least one design criterion.

Two preference aggregation rules satisfying these axioms have been investigated:

- Conservative ("weakest link") strategy:

$$\mu = \min({\mu_1}^{n_1},\ {\mu_2}^{n_2},\ \ldots,\ {\mu_{N_c}}^{n_{N_c}}) \tag{2}$$

where $n_i = w_i/w_{max}$, $i = 1, \ldots, N_c$, and w_{max} is the maximum of w_i over $i = 1, \ldots, N_c$, and w_i is a positive importance weight assigned to the i-th design criterion.

- Multiplicative trade-off strategy:

$$\mu = {\mu_1}^{m_1} {\mu_2}^{m_2} \ldots {\mu_{N_c}}^{m_{N_c}} \tag{3}$$

where $m_i = w_i / \sum_{j=1}^{N_c} w_j$, $i = 1, \ldots, N_c$, and w_i is a positive importance weight assigned to the i-th design criterion.

As already described, the importance weight assigned to each design criterion can be used to control its trade-off relative to the other criteria, that is, selected design criteria can be given more influence than others during optimization by assigning larger values to their importance weights. The choice of the values for these weights is subjective. The designer can gain experience with respect to their selection in any design problem by investigating the influence of different values of the weights on the final optimal design and on the corresponding preference values for each design criterion. For example, if the designer wishes to perform an "aggressive" code-based design which approaches close to the code drift limit (Figure 1), the importance weight for a building cost criterion, which will conflict with the code drift criterion, should be made much larger than the importance weights for the other design criteria. This will give greater emphasis to reducing costs during the trade-off in the optimization at the expense of giving a design which is closer to the code drift limit.

The importance weights w_i can be viewed from another perspective. Since there is no natural scale for preferences over all the diverse design criteria, there is a need to be able to independently control their influence during the trade-off which occurs in the optimization process. In the case that the w_i are all equal, the trade-off is governed by the inherent sensitivity of each μ_i with respect to $\boldsymbol{\theta}$. This "natural" trade-off may not satisfy the designer, who may want to give greater influence to selected criteria. In this case, an importance weight, say w_j, can be increased, then the sensitivity of μ_j with respect to $\boldsymbol{\theta}$ will be increased, which will give the j-th criterion more influence during the optimization.

Difficulties were encountered in performing the numerical optimization when the conservative strategy given in (2) was used. To give an example, consider the $\mu(\boldsymbol{\theta})$ surface shown in Figure 2 for this strategy, which is based on a three-story steel frame described later. For the surface plot, two design parameters were chosen: the flange width B and the web depth D for all the beams and columns, which are constrained to be identical I-beams. The surface is like an island of acceptable designs in a sea of unacceptable ($\mu = 0$) designs. The optimal design is given by the location of the highest peak on the island. For this problem, the $\mu = 0$ boundary of the island is given by a line for the larger values of B and D, a line B = constant, and a curve for the smaller values of B and D. These three boundary curves are due, respectively, to the zero preference value boundaries for the following three design criteria: low steel volume, bounded flange widths, and code-bounded lateral deflection under wind loads (there were no seismic loads applied for this illustrative example).

It can be seen from Figure 2 that the surface is characterized by sharp edges and the maximum value of $\mu(\boldsymbol{\theta})$ is at the intersection of these edges. The edges correspond to the equality of the preference functions for two design criteria, and they are transition curves where there is a switch in which design criterion is giving the smallest preference value, and so giving the value of the overall design evaluation measure, μ. These sharp edges in the $\mu(\boldsymbol{\theta})$ surface produced by the conservative strategy cause the difficulties encountered in performing the numerical optimization. For example, hill climbing algorithms move from a point on the surface corresponding to the initial choice of the design parameters up a sloping face until they reach the sharp ridge. After that, they are unable to efficiently move up the ridge to the peak value of the surface because of the discontinuous slope at the ridge. The stochastic optimization method described later can be applied because it requires only continuity, not differentiability, of the surface but convergence was rather slow. Apart from the numerical difficulties encountered during the optimization process, the conservative strategy, due to its focus on improving the worst aspect of the design, does not allow a full trade-off of conflicting criteria. Therefore, the conservative strategy is, in most cases, less desirable.

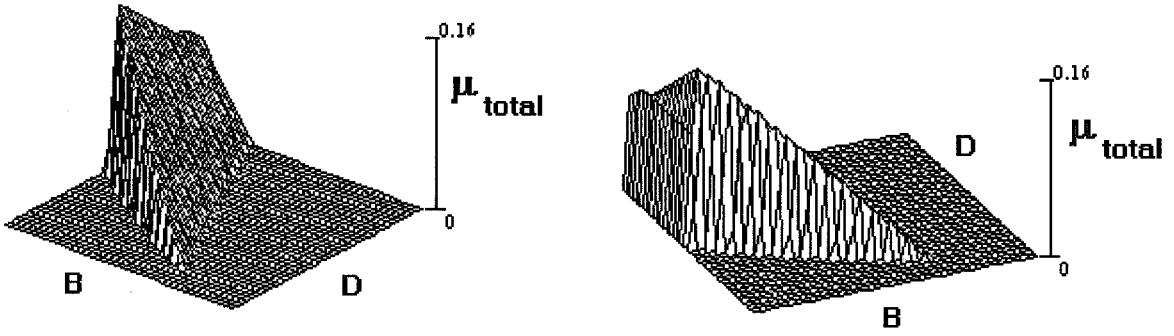

Figure 2: Surface $\mu(\boldsymbol{\theta})$ for the Conservative ("Weakest Link") Strategy

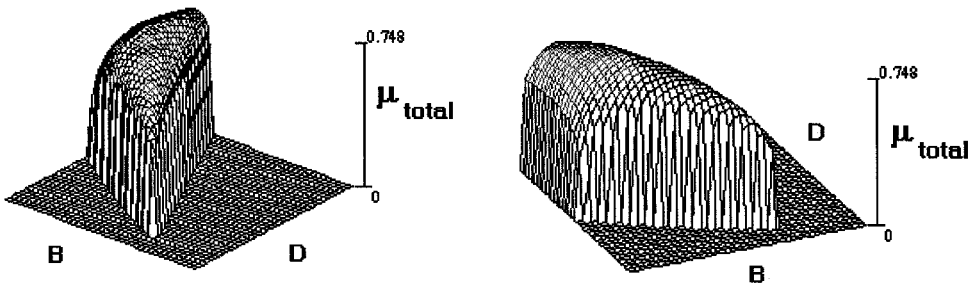

Figure 3: Surface $\mu(\boldsymbol{\theta})$ for the Multiplicative Trade-Off Strategy

As shown in Figure 3, the multiplicative trade-off strategy produces a $\mu(\boldsymbol{\theta})$ surface which does not have sharp edges. The plotted surface is for the same example as in Figure 2 except that (3) is used for the preference aggregation rule instead of (2). Notice that the $\mu(\boldsymbol{\theta})$ surface

in Figure 3 is very steep near the boundaries, which are the same $\mu = 0$ boundaries as in Figure 2. In fact, the slope of the surface at the boundaries is theoretically infinite. These steep boundary slopes cause hill climbing algorithms to quickly move towards the interior of the island if the algorithms are started near the boundary. Because of these desirable features, the multiplicative trade-off strategy is used in the examples presented later.

Special cases of the optimal design methodology based on the multiplicative trade-off strategy (3) can be related to existing optimal design concepts. For example, it is easily shown that the optimal solution obtained by maximizing (3) belongs to the Pareto optimal set corresponding to the multiple "objectives" $\mu_1, \ldots, \mu_{N_c}$ (Chan 1997). Also, consider the special case of the proposed methodology for which the preference function μ_i of the performance parameter q_i decreases monotonically with q_i so that $\frac{d\mu_i}{dq_i} < 0$. If a hard form of the preference functions is implemented in the design for all other design criteria, that is, for all $j \neq i$, $\mu_j = 1$ for $q_{j,l} \leq q_j \leq q_{j,u}$ and $\mu_j = 0$ otherwise, the unconstrained optimization problem in (3) is then equivalent to the constrained optimization problem in which $q_i(\boldsymbol{\theta})$ is minimized with respect to $\boldsymbol{\theta}$ while subject to the constraints $q_{j,l} \leq q_j(\boldsymbol{\theta}) \leq q_{j,u}, (j \neq i)$. This constrained optimization problem arises in existing optimal design methodologies involving the minimization of a cost or system failure probability subject to constraints on the reliability or cost respectively, together with other design constraints. For example, q_i could be the building cost and to reflect the fact that lower cost is preferred, the corresponding preference function μ_i of q_i would be chosen to decrease monotonically with q_i. Thus, the condition $\frac{d\mu_i}{dq_i} < 0$ would be satisfied. For reliability-based optimal design, a performance parameter q_j could then represent the structural failure probability which should be below a specified threshold $q_{j,u}$.

2.4 The Revision Stage

The iterative revision of the design to obtain a better, and eventually an optimal, design is a matter of solving an optimization problem using the overall design evaluation measure $\mu(\boldsymbol{\theta})$ from the evaluation stage as the objective function. Thus, it is necessary to develop a systematic procedure for generating a sequence of vectors $\boldsymbol{\theta}^0, \boldsymbol{\theta}^1, \ldots, \boldsymbol{\theta}^k, \ldots$, such that

$$\mu(\boldsymbol{\theta}^0) < \mu(\boldsymbol{\theta}^1) < \cdots < \mu(\boldsymbol{\theta}^k) < \cdots \tag{4}$$

and which converges to the maximum of μ. There are many methods for generating such a sequence of vectors, with each method having its own characteristics with regard to rate of convergence, extent of derivative information that is needed, stability considerations, ease of implementation, tendency of convergence to a local maximum, computational efficiency, etc. Practical optimization techniques have been receiving particular attention in structural optimization since realistic problems are often characterized by a high-dimensional design parameter vector and a multi-modal objective function whose evaluation at every single iteration step (out of a very large number) requires an extensive amount of computational effort (e.g. executing a general purpose finite-element code).

In structural design problems, the function $\mu(\boldsymbol{\theta})$ in (3) is usually defined over a discrete space of variables $\boldsymbol{\theta}$. For example, steel I-beam sections are available commercially in only a discrete set of sizes such as the W-shapes in the AISC list (AISC 1989). Thus, in this case,

the optimization involving member sizes as design parameters must be done over this discrete set. Genetic algorithms are useful for discrete optimization and in the CODA software, a new genetic algorithm called vGA has been implemented (Chan 1997). On the other hand, if the design parameters are defined in a continuous space, computationally efficient techniques for optimizing continuous functions can be used, such as adaptive random search (Masri et al. 1980) or a hybrid genetic algorithm (Chan 1997), both of which are well-suited for finding the global maximum of $\mu(\boldsymbol{\theta})$ in higher-dimensional design parameter spaces. A deterministic optimization approach, such as the quasi-Newton (variable metric) method (Press et al. 1986) can also be used (but primarily for lower-dimensional design parameter spaces). Of course, the optimal design may not always be unique but, in practice, it is sufficient if the optimization algorithm finds at least one global maximum.

In the examples presented later, the continuous optimizations are performed using adaptive random search. The basic algorithm proceeds as follows: (1) An initial parameter value $\boldsymbol{\theta}^0$ is chosen and $\mu(\boldsymbol{\theta}^0)$ is evaluated; (2) trial points $\boldsymbol{\theta}^i \in \Omega_\theta$, where Ω_θ is the given permissible region in the M-dimensional parameter space, are selected from an appropriate probability density function defined over Ω_θ; (3) a successful point $\boldsymbol{\theta}^{i+1}$ is one for which $\mu(\boldsymbol{\theta}^{i+1}) > \mu(\boldsymbol{\theta}^i)$. In general, convergence in probability is guaranteed, that is,

$$Prob\{|\boldsymbol{\theta}^n - \boldsymbol{\theta}^*| > \epsilon\} \to 0 \quad for \;\; n \to \infty \tag{5}$$

where $\boldsymbol{\theta}^*$ is an optimal parameter value. This is a weak form of convergence but it applies even in the presence of multiple maxima and nondifferentiability of $\mu(\boldsymbol{\theta})$.

Instead of using "pure random search", a "random creep" procedure is used in which exploratory steps are confined to a hypersphere centered about the latest successful point $\boldsymbol{\theta}^i$. However, convergence may be slow if no allowance is made for variations in the nature of the objective function surface. Therefore, the adaptive random search algorithm periodically optimizes the variance of the step-size distribution (Masri et al. 1980). By searching over a variance range of many decades, the algorithm finds the step-size distribution that yields the best local improvement in the criterion function. The variance search is then followed by a specified number of iterations of local random search where the step-size variance remains fixed. Periodic wide-range searches are introduced to ensure that the process does not stop at a local maximum.

3 TREATMENT OF UNCERTAINTIES

Predictions of structural response have to account for modeling errors and the uncertain loads that the completed structure will experience during its lifetime. The performance of the structure is usually judged in this case by safety considerations and a measure of safety is provided by component and system reliability. For example, the peak interstory drift over the lifetime of the structure due to earthquakes is uncertain. Thus, a performance parameter can be chosen to be directly related to the interstory drift reliability. In the analysis stage, available probabilistic analysis tools are then used to calculate the structural reliability or, equivalently, the failure probability, corresponding to a specified interstory drift limit.

The first step in developing an expression for the probability of structural failure, designated by $F(\boldsymbol{\theta})$ for a design corresponding to $\boldsymbol{\theta}$, is to characterize the seismic hazard at the construction site by a set of ground motion parameters $\boldsymbol{\alpha}$ (for example, peak ground acceleration, response spectrum ordinates, duration of motion, frequency content, etc.). For most probabilistic hazard models in use, these parameters depend, through appropriate "attenuation" relationships, on a set of uncertain "seismicity" variables, which are designated here by a vector $\boldsymbol{\phi}$ and which account for the uncertain regional seismic environment. For example, $\boldsymbol{\phi}$ may include variables such as earthquake magnitude, fault dimensions, source parameters, epicentral distance, propagation path properties and local site conditions. The uncertain values of $\boldsymbol{\phi}$ are described by a probability density function $p(\boldsymbol{\phi})$. For example, $p(\boldsymbol{\phi})$ might be chosen to model the probability of occurrence of an earthquake of a given magnitude and the probability of fault rupture at specific locations along a fault.

The required attenuation relationships are often derived by an empirical fit to the observed data. There is uncertainty associated with these attenuation models, even when $\boldsymbol{\phi}$ is known, which is reflected by the scatter of the analyzed data about the mean or median model predictions. Therefore, the attenuation relationship should actually give a probabilistic description $p(\boldsymbol{\alpha} \mid \boldsymbol{\phi})$ of the relation between the ground motion parameters $\boldsymbol{\alpha}$ and the seismicity parameters $\boldsymbol{\phi}$.

Knowing the ground motion parameters $\boldsymbol{\alpha}$ for a site does not completely specify the structural excitation. Furthermore, because of the presence of modeling errors, the structural model corresponding to a particular design $\boldsymbol{\theta}$ will not accurately predict the response of the structure should it be built. These uncertainties mean that a failure probability corresponding to a design $\boldsymbol{\theta}$ which is conditional on the ground motion parameters, designated by $F(\boldsymbol{\theta} \mid \boldsymbol{\alpha})$, must be set up. This can be done using probabilistic analysis tools. For example, the effect of the uncertainty in the seismic excitation at the site can be treated using random vibration analysis if the ground motion is modeled as a stochastic process depending on the parameters $\boldsymbol{\alpha}$. On the other hand, stochastic finite-elements or other methods for uncertain dynamical systems could be used to treat the modeling uncertainties (e.g. Der Kiureghian and Ken 1988, Spanos and Ghanem 1989, Deodatis 1991, Katafygiotis and Papadimitriou 1996, Papadimitriou, Beck, and Katafygiotis 1995, 1997).

Finally, the uncertainties in the seismic environment, ground motion modeling and structural modeling can be combined using the total probability theorem to determine the total failure probability given the occurrence of an earthquake event

$$F(\boldsymbol{\theta}) = \int_{\boldsymbol{\phi}} \int_{\boldsymbol{\alpha}} F(\boldsymbol{\theta} \mid \boldsymbol{\alpha})\, p(\boldsymbol{\alpha} \mid \boldsymbol{\phi})\, p(\boldsymbol{\phi})\, d\boldsymbol{\alpha}\, d\boldsymbol{\phi} \tag{6}$$

The failure probability over the lifetime of the structure is then computed using an occurence model for earthquake events. Assuming that the occurences of earthquakes follow a Poisson arrival process, the probability that the structural safety requirements are not satisfied during the lifetime t years of the structure, is given by:

$$F_{life}(\boldsymbol{\theta},\ t) = 1 - \exp[-\nu\ F(\boldsymbol{\theta})\ t] \tag{7}$$

where $F(\boldsymbol{\theta})$, given in (6), is the failure probability given the occurrence of an event, and ν is the expected number of events per annum.

4 RELIABILITY COMPUTATIONS

It is reasonable to evaluate the multi-dimensional integral (6) numerically only if the dimension is low. Otherwise, efficient importance sampling simulation methods (Schuëller and Stix 1987, Bucher 1988, Papadimitriou, Beck, and Katafygiotis 1997, Au et al. 1998) or asymptotic methods (Papadimitriou, Beck, and Katafygiotis 1995, 1997) must be used. Asymptotic methods are used in this work to compute the multi-dimensional probability integrals as follows.

Consider first the case for which the conditional reliability function $F(\boldsymbol{\theta} \mid \boldsymbol{\alpha})$ is a smooth function of $\boldsymbol{\alpha}$. This case is encountered when the excitation is modeled by parametric stochastic processes with parameters $\boldsymbol{\alpha}$ and/or when model error is quantified probabilistically and accounted in the model response prediction. For fixed values of $\boldsymbol{\alpha}$, the failure probability can be computed using available random vibration results (Lin 1967, Lutes and Sarkani 1997) and/or probabilistic analysis tools which treat the model error. Using the method developed by Papadimitriou, Beck, and Katafygiotis (1997) for integrals of the type (6), an asymptotic approximation of the value of the integral is

$$F(\boldsymbol{\theta}) \sim \sum_{i=1}^{k} (2\pi)^{n/2} \frac{F(\boldsymbol{\theta} \mid \boldsymbol{\alpha}_i^*)\, p(\boldsymbol{\alpha}_i^*,\ \boldsymbol{\phi}_i^*)}{\sqrt{\det L(\boldsymbol{\alpha}_i^*,\ \boldsymbol{\phi}_i^*)}} \tag{8}$$

where $L(\boldsymbol{\alpha},\ \boldsymbol{\phi}) = -\nabla\nabla\ell(\boldsymbol{\alpha},\ \boldsymbol{\phi})$ is the Hessian matrix of $-\ell(\boldsymbol{\alpha},\ \boldsymbol{\phi})$, defined by

$$\ell(\boldsymbol{\alpha},\ \boldsymbol{\phi}) = \ln F(\boldsymbol{\theta} \mid \boldsymbol{\alpha}) + \ln\ p(\boldsymbol{\alpha},\ \boldsymbol{\phi}) \tag{9}$$

and $(\boldsymbol{\alpha}_i^*,\ \boldsymbol{\phi}_i^*)$ are the local multiple maxima of the integrand in (6) with respect to $\boldsymbol{\alpha}$ and $\boldsymbol{\phi}$. The optimization method developed by Yang and Beck (1998) can be used to search and locate the multiple maxima. Often, there is a single maximum and therefore there is only one term contributing in (8). Importance sampling methods can also be used to improve, whenever desirable, the value of the estimate in (8). Efficient implementation of importance sampling method is based on the knowledge of the global and, whenever applicable, the local multiple maxima $(\boldsymbol{\alpha}_i^*,\ \boldsymbol{\phi}_i^*)$, as well the asymptotic contribution from each local maximum given by each term in (8). Applications of the asymptotic approximation (8) to earthquake engineering and reliability-based optimal structural control design can be found in Papadimitriou, Katafygiotis, and Au (1997) and May and Beck (1998).

Other methods available in the literature to approximate (6) are the ones proposed by Igusa and Der Kiureghian (1988) and Cherng and Wen (1994) which require first the transformation of the integral into the classical reliability integral and then the application of the FORM or SORM approximations to the transformed integral. The reader is referred to the work by Papadimitriou, Beck, and Katafygiotis (1997) for a discussion of the differences between the various methodologies and the advantages and disadvantages of the present formulation for the type of probability integrals (6) for which $F(\boldsymbol{\theta} \mid \boldsymbol{\alpha})$ is a smooth function of $\boldsymbol{\alpha}$.

In the case where only $\boldsymbol{\alpha}$ and $\boldsymbol{\phi}$ are uncertain, that is, the load of the structure is completely specified for given $\boldsymbol{\alpha}$ and $\boldsymbol{\phi}$, the domain in the space of parameters $\boldsymbol{\alpha}$ and $\boldsymbol{\phi}$ is divided into safe and unsafe domains depending on whether $F(\boldsymbol{\theta} \mid \boldsymbol{\alpha})$ takes the value 0 or 1 in these

domains, respectively. First, consider the case of component reliability for which there is a single failure surface, typically given in the implicit form $g(\boldsymbol{\alpha},\ \boldsymbol{\phi}) = 0$, separating the safe and unsafe regions in the variable space $(\boldsymbol{\alpha},\ \boldsymbol{\phi})$. The safe and unsafe domains are defined as $\mathcal{S} = \{\boldsymbol{\alpha},\ \boldsymbol{\phi} \in \mathbb{R}^n : g(\boldsymbol{\alpha},\ \boldsymbol{\phi}) > 0\}$ and $\mathcal{F} = \{\boldsymbol{\alpha},\ \boldsymbol{\phi} \in \mathbb{R}^n : g(\boldsymbol{\alpha},\ \boldsymbol{\phi}) < 0\}$, respectively. The failure probability integral (6) can be transformed to an integral over the failure domain in the space $\boldsymbol{\alpha}$ and $\boldsymbol{\phi}$ variables. The probability of failure becomes

$$F(\boldsymbol{\theta}) = \int_{g(\boldsymbol{\alpha},\ \boldsymbol{\phi})<0} p(\boldsymbol{\alpha},\ \boldsymbol{\phi})\, d\boldsymbol{\alpha}\, d\boldsymbol{\phi} \tag{10}$$

This reliability integral can be evaluated approximately using available FORM/SORM methods (e.g. Madsen et al. 1986, Der Kiureghian et al. 1987, Breitung 1989, Papadimitriou, Beck, and Katafygiotis 1997, Polidori et al. 1998). Response surface methods (Faravelli 1989) can also be used to evaluate the integral in (10).

To simplify computations and avoid the computational expensive transformation of variables to the standard Normal space, which is required in some FORM and SORM methods, the evaluation of the integral in the proposed formulation will be based on asymptotic expansions developed in the original space of random variables. One such expansion has been proposed by Breitung (1991). A simpler asymptotic expansion well-suited for approximating the integral in the original space has recently been developed by Polidori et al. (1998). Specifically, let φ denote one of the variables in the set $(\boldsymbol{\alpha},\ \boldsymbol{\phi})$ and $\boldsymbol{\psi}$ denote the remaining $m = n-1$ variables in the same set. Starting with the assumptions that the variable φ is independent of the others so that $p(\boldsymbol{\psi},\ \varphi) = p(\boldsymbol{\psi})p(\varphi)$, and the assumption that the failure surface $g(\boldsymbol{\alpha},\ \boldsymbol{\phi}) \equiv g(\boldsymbol{\psi},\ \varphi) = 0$ can be written in the explicit form $\varphi = h(\boldsymbol{\psi})$, the n-dimensional failure probability integral over the unsafe region in the space $(\boldsymbol{\alpha},\ \boldsymbol{\phi})$ can be rewritten as an $m = n - 1$ dimensional probability integral

$$F(\boldsymbol{\theta}) = \int_{\mathbb{R}^m} P_\varphi(h(\boldsymbol{\psi}))p(\boldsymbol{\psi})d\boldsymbol{\psi} \tag{11}$$

over the whole space of variables $\boldsymbol{\psi}$, where

$$P_\varphi(h(\boldsymbol{\psi})) = \int_{-\infty}^{h(\boldsymbol{\psi})} p(\varphi)\, d\varphi \tag{12}$$

and $P_\varphi(\cdot)$ is the cumulative distribution function for the random variable φ. Note that $P_\varphi(y)$ involves computing a one-dimensional integral over φ, which, depending on the form of $p(\varphi)$ can be carried out either analytically or numerically. Applying the asymptotic approximation proposed by Papadimitriou, Beck, and Katafygiotis (1997) for this type of integral gives

$$F(\boldsymbol{\theta}) \sim \sum_{i=1}^{k} (2\pi)^{m/2}\, \frac{P_\varphi(h(\boldsymbol{\psi}_i^*))\, p(\boldsymbol{\psi}_i^*)}{\sqrt{\det L(\boldsymbol{\psi}_i^*)}} \tag{13}$$

where $L(\boldsymbol{\psi}) = -\nabla\nabla\ell(\boldsymbol{\psi})$ and $\ell(\boldsymbol{\psi}) = \ln P_\varphi(h(\boldsymbol{\psi})) + \ln p(\boldsymbol{\psi})$. Multiple maxima can be handled by summing the contributions from each maximum. The new method requires solving an

$(n-1)$–dimensional unconstrained minimization problem, while Breitung's method requires solving an n–dimensional constrained minimization problem. The formulation for the more general case which does not involve the assumptions of independence of φ from the other variables and the existence of the explicit relationship $\varphi = h(\boldsymbol{\psi})$ can be found in the work by Polidori et al. (1998).

Consider next the case for which there are multiple components, each with a failure surface defining the component's failure and that system failure occurs when any one of multiple components fails, that is, the system is inside one of the unsafe regions defined by each component failure surface. Let $g_i(\boldsymbol{\alpha},\ \boldsymbol{\phi}) = 0$ be the equation for each failure surface. The unsafe domain is the union of the unsafe domains defined from each such surface. The reliability integral (6) becomes

$$F(\boldsymbol{\theta}) = \int_{\bigcup_{i=1}^{n} g_i(\boldsymbol{\alpha},\ \boldsymbol{\phi})<0} p(\boldsymbol{\alpha},\ \boldsymbol{\phi})\, d\boldsymbol{\alpha}\, d\boldsymbol{\phi} \tag{14}$$

which is in the form of the classical reliability for a series system. This type of reliability for a series system is encountered in design when, for example, design criteria specify upper limits on the maximum lifetime drift at each story. The limit surface $g_i(\boldsymbol{\alpha},\ \boldsymbol{\phi}) = 0$ in this case is the interstory drift requirement for the i-th floor.

Simplified approximations to the reliability integral (14) can be given in several cases, provided certain conditions apply. One approximation is to replace the reliability integral by the sum of the component reliability integrals, that is, summing the contributions from each surface, which works well if the contribution from the overlapping failure domains is insignificant. Another approximation is to consider the contribution from the failure surface with the highest failure probability while neglecting the contributions from the other surfaces. This will yield a good approximation if the contribution from the other failure surfaces is insignificant or if the significant parts of the failure domains of the other surfaces are subsets of the failure domain of the failure surface with the highest failure probability. Such approximations will be considered later in the examples where their applicability is justified based on the results obtained.

In a more general case, the reliability of the structure can be estimated by modeling the structure by a series system where the elements in the series system are parallel systems. For a more formal study of such system reliability issues the reader is referred to the books by Madsen et al. (1986) and Thoft-Christensen and Murotsu (1986). These general system reliability approaches could readily be integrated, on an as-needed basis, with the multi-decision optimal design framework presented in this work.

5 IMPLEMENTATION OF THE OPTIMAL DESIGN METHODOLOGY

5.1 The CODA Software

The performance-based multi-criteria optimal design methodology has been implemented in a software package called CODA so that applications of the methodology can be investigated.

In CODA, there is a separate module for each of the three stages, namely, analysis, evaluation and revision stages, of the formal design procedure explained earlier. These modules are called the ANALYZER, the EVALUATOR, and the REVISER, respectively, and the operation of these modules is integrated under the control of a supervisory module, the EXECUTIVE. Figure 4 illustrates the connections between the four modules. The basic methodology for the automated optimal design process is implemented by repeated calls to the ANALYZER, EVALUATOR and REVISER by the EXECUTIVE.

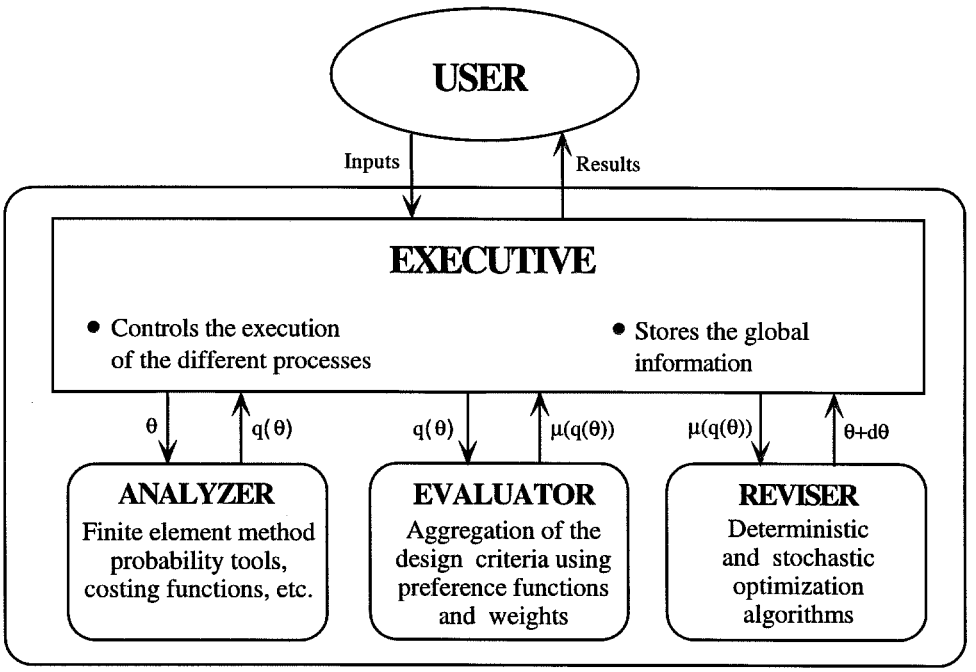

Figure 4: Modules of CODA

The ANALYZER uses finite element analysis techniques to compute structural performance parameter values based on a building configuration specified by the user and on the current values of the design parameters; the EVALUATOR then aggregates preference values for the current design, which are based on how well each of the individual design criteria are satisfied, in order to determine an overall evaluation measure for the design; and finally, the REVISER performs revisions of the design in order to find an optimal design based on maximization of the overall design evaluation measure. The EXECUTIVE acts as an interface between the user and the other three modules, assisting in their initialization, controlling their execution, performing error-checking and error-recovery, and storing and displaying the information associated with the analysis, evaluation and optimization.

The ANALYZER, EVALUATOR and REVISER modules are initialized by the user interacting with the EXECUTIVE. The user is prompted to input the basic physical configuration of the initial design and the geometric information of individual members and to specify member connection information. In addition, the user must select, from a menu of different choices,

the design and performance parameters to be considered during the design decision-making process. These design and performance parameters are combined with preference functions and importance weights to express the design criteria in the manner described earlier.

The principal role of the ANALYZER is to calculate the performance parameters $\mathbf{q}(\boldsymbol{\theta})$ as a function of the current design parameters, $\boldsymbol{\theta}$. The evaluation of a potential design is then made in the EVALUATOR using user-supplied preference functions, μ_i, $i = 1, \ldots, N_c$, where N_c is the number of design criteria. The preference functions are established by the user interacting with the EXECUTIVE. In the final stage of each iterative cycle, the REVISER takes the overall design evaluation measure, μ, computed by the EVALUATOR from the individual preference function values, μ_i, $i = 1, \ldots, N_c$, using the multiplicative trade-off preference aggregation rule and revises the design to improve it. The user may choose to perform a one-step revision of the current design, or to fully optimize the design. In the latter case, the EXECUTIVE cycles through the ANALYZER, EVALUATOR and REVISER until convergence to an optimal design is achieved or until a specified maximum number of cycles is reached.

5.2 Basic Modules of CODA

CODA was developed using object-oriented programming, a style of programming that establishes objects to represent and organize the information utilized by the program (Dym and Levitt 1991). CODA was implemented in this style to ensure that the code is modular and extensible. Modularity of the program was essential during software development since the project involved a collaborative effort between three universities. The ANALYZER module was developed at Stanford University; the EVALUATOR and EXECUTIVE were developed at the California Institute of Technology; and the REVISER was developed at the University of Southern California. Extensibility was also deemed important so that additional features and modules could be readily incorporated or modified after the completion of the initial prototype software. The ability to do this without having to restructure the entire software package greatly enhances programming efficiency.

Computer requirements to run CODA include the Windows NT or 95 operating systems, 16Mb of RAM, and approximately 10Mb of available disk space. The program was developed primarily using the Microsoft Visual C++ Development System for Windows.

5.2.1 The EXECUTIVE

As discussed previously and shown in Figure 4, the role of the EXECUTIVE is to initialize and to control the execution of the various processes, to perform error-checking and error-recovery and to store the information shared by the other modules (the ANALYZER, the EVALUATOR and the REVISER). This centralization eliminates the need for information protocols to pass data between the different modules of the program. The information is stored in the EXECUTIVE in C++ classes which can be accessed from each of the modules. These classes relate to: General Building Description; Building Members; Building Connections; Building Units; Design Criteria; Analysis Parameters and Optimization Parameters.

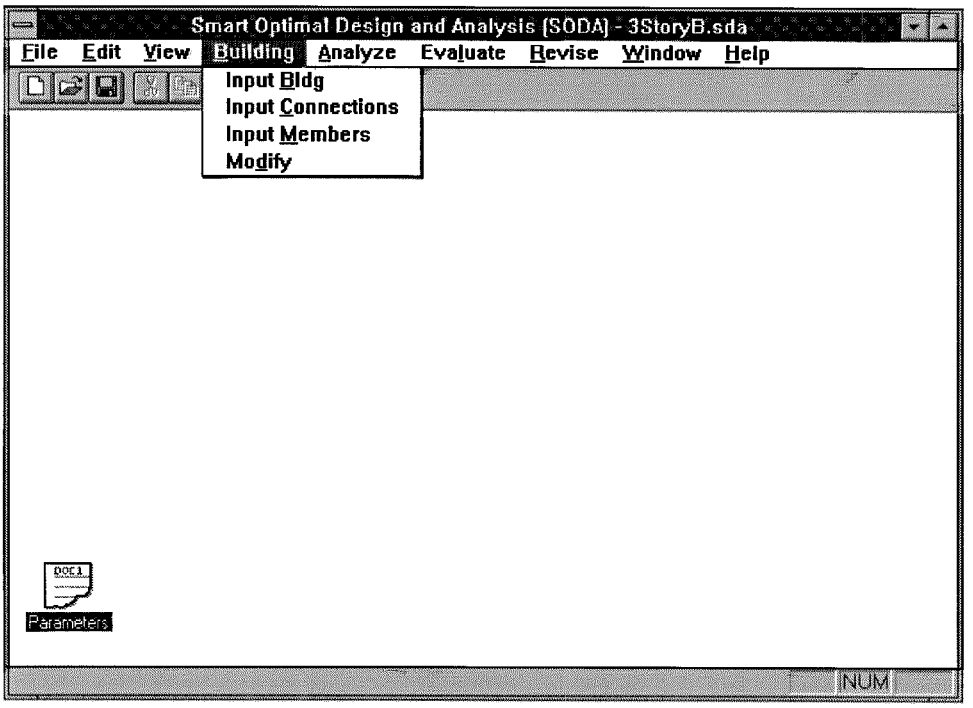

Figure 5: BUILDING Menu Items

The user interacts with CODA through the EXECUTIVE by choosing different menu options and entering information through dialog boxes (Beck et al. 1996a). For example, the *Building* menu item shown at the top of Figure 5 allows the user to input the general configuration of the proposed design including connection type and location, as well as member configuration and location. Each of these steps are done via dialog boxes which can be invoked by choosing the appropriate item inder the *Building* menu.

Also, as shown in Figure 6, using the *Analyze* menu, the user may define the design parameters, create the finite element model from the prescribed building model, define the design loads to be applied to the building model, and perform a single finite element analysis to compute the response, and so the performance parameters, for the current values of the design parameters. The dialog box for the *Define Design Parameters* command is illustrated in Figure 7. Structural loadings are input via the *Define Loads* command, where a combination of *Gravity, Earthquake, or Wind* can be specified. Once the building parameters have been input and the loadings have been defined, an analysis method is chosen (either modal, linear static, or linear dynamic) using the *Run Analysis* menu option.

As shown in Figure 8, through the *Evaluate* menu, the user can specify the criteria for evaluating a design and specify the corresponding performance parameters, as well as perform a single evaluation of the current design. To specify performance parameters, the user can choose from predefined performance quantities using the *Define Performance Parameters* command, as illustrated in Figure 9.

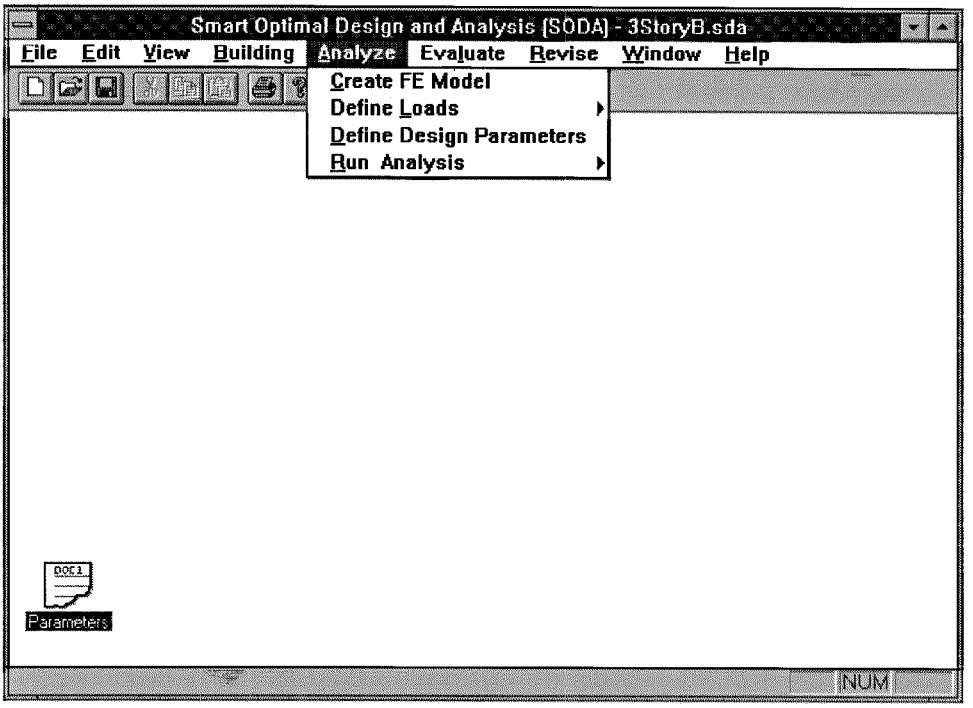

Figure 6: ANALYZE Menu Items

In addition to controlling all of the software processes and storing the analysis and design information, the EXECUTIVE allows the user to display intermediate and final results through the *View* menu (Figure 10). For example, a graphical representation of the finite element model can be displayed after its creation. Also, under the *View* menu, tabular listings can be displayed of the initial and revised (or optimal) design parameters, the corresponding performance parameters and preference function values, μ_i, for each design criterion, and the overall design evaluation measure, μ.

The EXECUTIVE contains several important classes. The primary class that stores all of the data and the member functions (subroutines) associated with each of the menu items is the *CCureeDoc* class. The *CCureeDoc* class was derived from the Microsoft Foundation Class *CDocument* which has several useful built-in member functions and attributes. The *CMainFrame* class defines the main window and menu of the application, while the *CCuree* class is used to initialize many of the overall parameters. Additional classes in the EXECUTIVE display information and results to the user. For example, *CCureeView*, *CResView*, and *CModelView* are used to display the initialization parameters, results and finite element model, respectively. Other classes in the EXECUTIVE are used to open dialog boxes for user input.

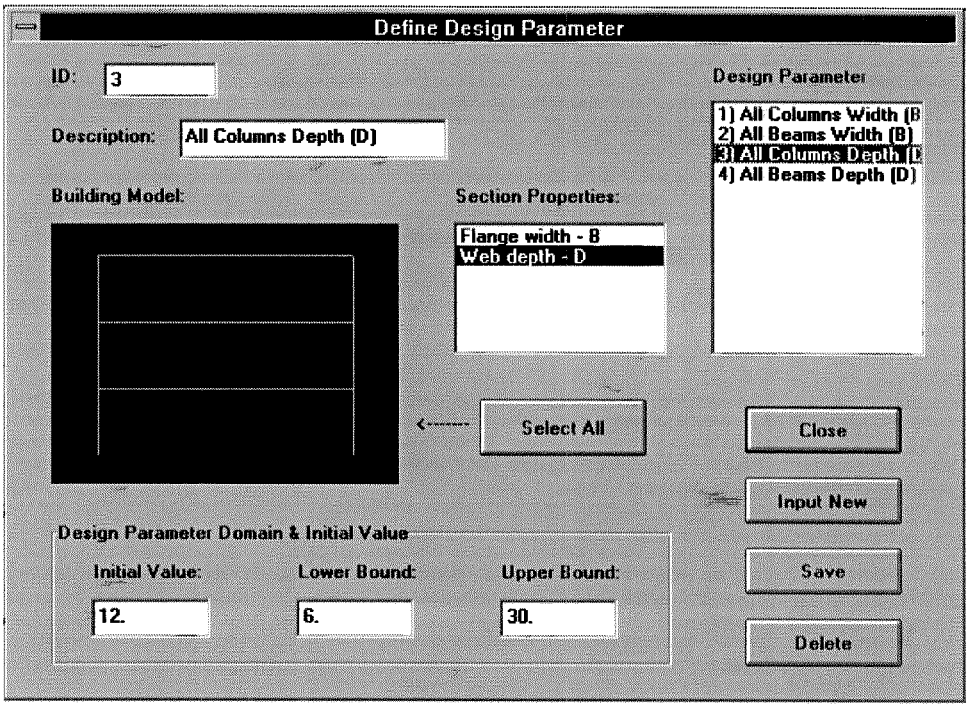

Figure 7: Defining Design Parameters

5.2.2 The ANALYZER

The role of the ANALYZER is to compute performance parameter values corresponding to the current values of the design parameters. The performance parameters include steel volume, base shear, maximum displacement, individual and maximum interstory drifts, member axial, shear and bending stresses, and component and system reliabilities. Steel volume is a proxy for material cost. It is computed by summing up the volume of all of the members. The other performance parameters currently considered in CODA are computed using basic finite element methods. The current version of CODA can perform static and dynamic linear finite element analysis of planar frames. Frame members may be modeled as either beam-column or truss elements. The stiffness matrix of the individual elements are computed, converted to global coordinates, and assembled into a system stiffness matrix using conventional finite element procedures. "Lumped" mass finite element matrices are created for use in dynamic analyses.

For static design loads, the user can consider gravity (dead and live) loading as well as earthquake and wind loading. The gravity loading is defined by the user as load/unit area; separate values may be entered for both the roof and floor dead and live loads. The dead and live loads are multiplied by the tributary area to determine the actual load vector values. The wind load is based on the 1994 Uniform Building Code (UBC) prescribed loading (ICBO 1994). The required parameters to compute the code-based wind pressure may be input by the user. Default values are also supplied based on the UBC. The wind pressure is multiplied

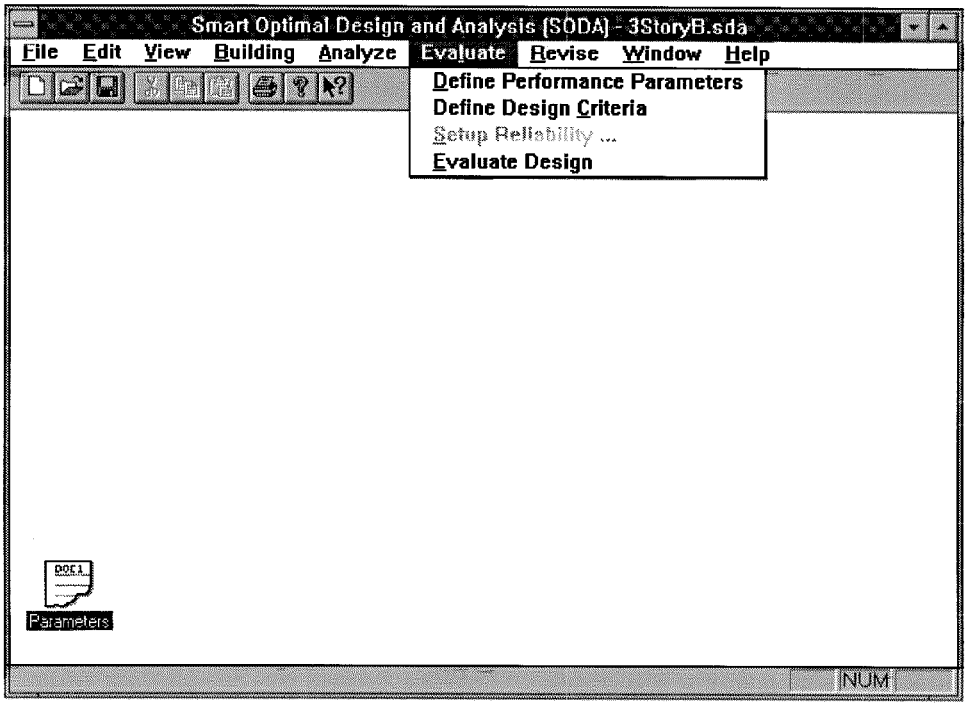

Figure 8: EVALUATE Menu Items

by the tributary area to determine the actual load vector values.

Earthquake engineering analyses can be performed using either static UBC loadings, the response spectrum method, or linear time-domain integration techniques. The equivalent static lateral force procedure is based on the 1994 UBC prescribed loading pattern, that is, the design base shear is distributed to each floor of the building according to the appropriate UBC formula (ICBO 1994). This distributed base shear forms the static load vector which is used to compute the building displacements, member stresses, etc. For these static earthquake design loads (as well as gravity or wind loads), LU Decomposition is used to solve for the nodal displacement. The subroutines used in CODA for this decomposition are modified versions of those found in Press et al. (1986). Once the nodal displacements have been computed, additional results including interstory drift values, base shear, and structural member forces and stresses, may be computed.

Seismic response can also be calculated using the response spectrum method, based on modal superposition, calculation of modal participation factors, and the UBC design response spectrum. An eigenvalue analysis is first performed using the Jacobi transformation method (Press et al. 1986). Structural damping is input through user-specified modal damping ratios. The ANALYZER is also capable of performing linear time-domain integration using the average and linear acceleration Newmark-Beta algorithms.

In the software implementation of the ANALYZER, the main class created is *Analysis*. The following information is included in this class: Finite Element Model; Load Vector; Mass and

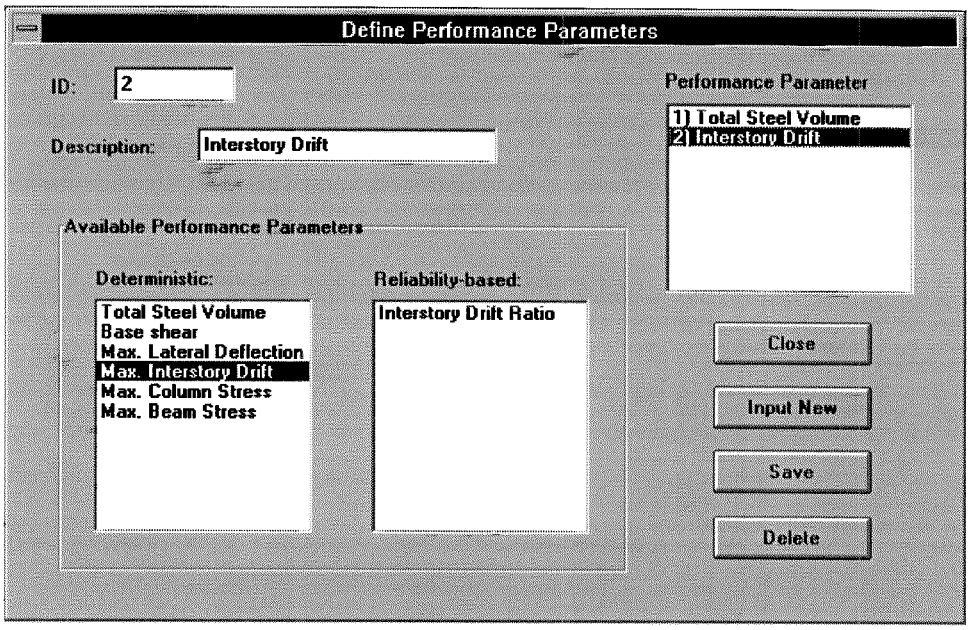

Figure 9: Defining Performance Parameters

Stiffness Matrices; Gravity, Wind, and Earthquake Loads; Modal Properties; and Results. Much of this information is stored in separate subclasses within the *Analysis* class. For example, subclass *Results* contains the values of the performance parameters: Steel Volume, Maximum Deflections and Drift, Maximum Column and Beam Axial, Shear, and Bending Stresses, and Lifetime Interstory Drift Reliability. The *Analysis* class also contains member functions which perform the finite element analysis (Beck et al. 1996a).

5.2.3 The EVALUATOR

The task of the EVALUATOR is to provide an overall design evaluation measure $\mu(\boldsymbol{\theta})$ for the design specified by the current value of the design parameter vector $\boldsymbol{\theta}$. The measure $\mu(\boldsymbol{\theta})$ serves as an objective function which the REVISER uses to determine improved, or optimal, designs.

To evaluate the design, the EVALUATOR performs the required operations as explained in the section on the evaluation stage of the optimal design methodology. Namely, through preference functions, the EVALUATOR incorporates the performance parameter values obtained in the ANALYZER into the overall design measure using the multiplicative trade-off strategy to allow trading-off of conflicting criteria.

In the software implementation of the EVALUATOR, the main class which was created is *Evaluate*. This performs certain duties and stores the following information: a list of design criteria; the overall design evaluation measure μ; and the method to compute μ. Each design criterion is an object in a class called *Criteria*. Each object of this class holds the following information: a linked-list that holds performance (or design) parameters associated

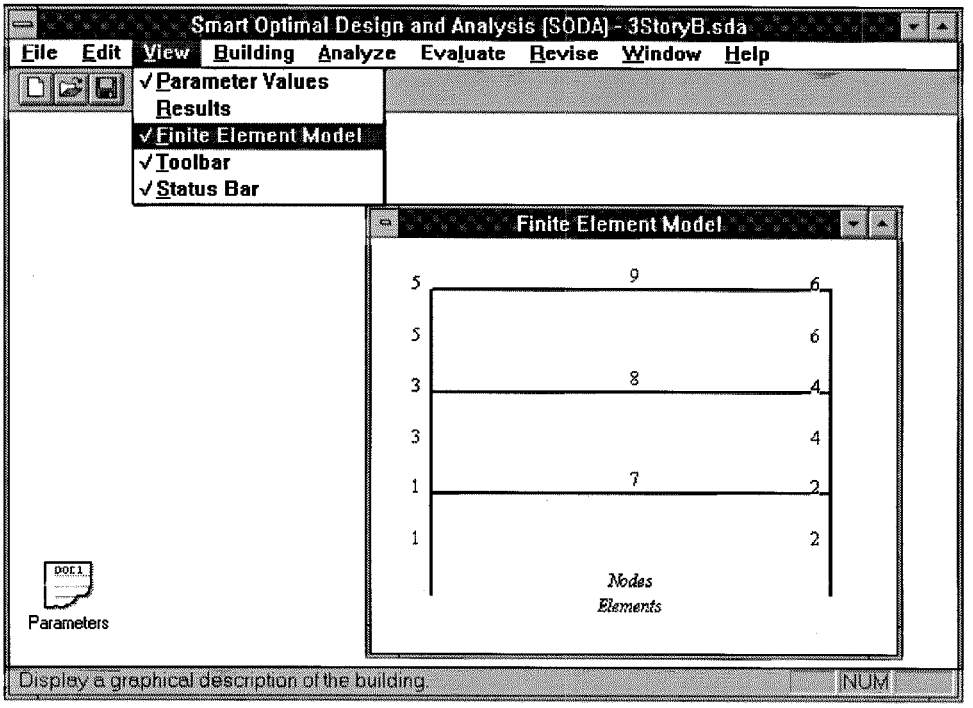

Figure 10: Viewing the Finite Element Model

with the criterion; the method to setup this linklist; preference function value μ_i; the method to compute μ_i; and the importance weight w_i.

To handle information about the design and performance parameters, two classes, *Theta* and *Performance*, are defined. A *Theta* object contains the following information about a design parameter: ID number (j) and description of the parameter; initial and revised values of the design parameter θ_j; upper and lower bounds of the parameter θ_j; type of group to allow linking to give a common value with other design parameters; a linked-list that holds all building members grouped with this design parameter; the type of design parameter, such as flange width or web depth. Grouping of building members for a design parameter can be done in terms of story units. For a particular story of a building model, one can specify all the beams, all the columns, or all beams and columns in that story as a group for the design parameter. Alternatively, one can define a group based on all the beams, all the columns, or all the members in the entire building.

Similarly, an object of the *Performance* class contains the following information about a performance parameter: ID number (k) and description of the parameter; performance type; and performance value q_k. Currently, several performance types are available. They include total steel volume, maximum base shear, maximum lateral deflection, maximum interstory drift, individual interstory drifts, maximum beam stress and maximum column stress, and an interstory drift failure probability. The performance value q_k is taken from the *Results* object defined in the *Analysis* object.

Another class called *PrefFunc* is created to store information that defines a preference function. Each object contains the following information: the type of preference function (four types are defined); the array of parameters that define the function; and a function that computes the preference value for the current calculated performance parameter value or design parameter value.

5.2.4 The REVISER

The REVISER module of CODA houses various choices of optimization techniques for the unconstrained maximization problem arising in the design methodology: a quasi-Newton method, an adaptive random search method and two genetic algorithms. For discrete optimization, a genetic algorithm called vGA can be chosen. For continuous optimization, one of the other three techniques can be chosen, namely, adaptive random search or a hybrid genetic algorithm as stochastic optimization options, or the quasi-Newton variable metric method for deterministic optimization.

The REVISER module is primarily made up of three C++ classes: *Revise* and its two subclasses, *QnmOpt* and *StochOpt*, which encapsulate the optimization algorithms. The *Revise* class has a *virtual function* called *Optimize*. This class member function calls the user-selected optimization scheme at run-time without using *if – else if* statements. The virtual function allows new optimization algorithms to be added to CODA without changing the internal structure of the REVISER module.

6 EXAMPLE I

6.1 Structural Model and Design Criteria

The optimal design methodology is demonstrated by applying it to the design of a three-story, single-bay moment-resisting frame. The frame members are taken as steel I-beams with the length of the floor beams fixed at 240 inches and the height of the story columns fixed at 120 inches. The connections are modeled as rigid. Gravity loads are taken as 60 lb/ft^2 and 50 lb/ft^2 for the dead and live loads, respectively for each floor and the roof. An out-of-plane tributary width of 100 inches is used for the gravity load calculations.

Both continuous and discrete cases of the design parameter space are considered. The design parameters $\boldsymbol{\theta}$ in the continuous case are member flange width B and web depth D for the beams and columns. The two design parameter sets considered are: $\boldsymbol{\theta} = (B,\ D)$, where the beams and columns are required to have the same cross-sectional dimensions, and $\boldsymbol{\theta} = (B_{beam},\ D_{beam},\ B_{col},\ D_{col})$, where the beams and columns are free to have different cross-sectional dimensions. The flange and web plate thicknesses are held fixed at 0.25 inches. In the continuous case, the adaptive random search algorithm, described earlier, is used to obtain the optimal design. In the discrete case, the vGA genetic algorithm is used (Chan 1997) and the optimization is performed over a subset of 128 of the AISC W-shapes (AISC 1989).

The objective is to determine $\boldsymbol{\theta}$ so that the frame design is optimized according to design criteria involving the following performance parameters: flange width, web depth, building cost, probability of unacceptable peak lifetime interstory drift (drift risk), and code-based maximum interstory drift and maximum allowable stresses in structural members. The importance weight for each design criterion is set to 1.0 for the aggregation of preference values in equation (3), unless otherwise stated. The corresponding preference functions are shown in Figure 11.

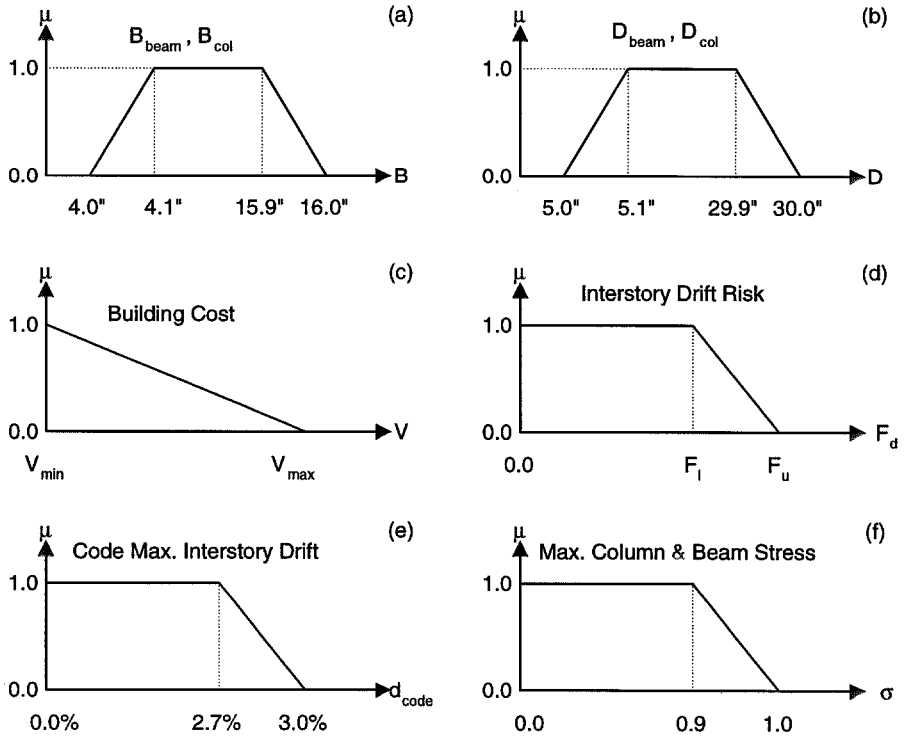

Figure 11: Preference Functions for Different Performance Parameters

The first two design criteria shown in Figure 11(a) and (b) involve "soft" constraints on the design parameters, so the preference functions define constraints on cross-sectional dimensions of the structural members. Specifically, the forms of the preference functions show that, for example, in the case of flange width B, members with flange widths shorter than 4.0 inches or longer than 16.0 inches are unacceptable, while those with flange widths between 4.1 to 15.9 inches are favored the most. Flange widths between 4 to 4.1 inches and 15.9 to 16.0 inches have various intermediate degrees of acceptance or satisfaction. One can interpret the preference function for the web depth D of the structural members in a similar way. In real-life applications, the sizes defining the shape of the preference functions related with the cross-sectional dimensions of structural members might be dictated, for example, by the limited availability of structural elements in stock or by architectural restrictions imposed on the

structure. It should be noted that, since there is no "uncertainty" about the member sizes once they are chosen, the preference values for them can be computed and incorporated in the preference aggregation rule (3) directly.

The preference function for the building cost is given in Figure 11(c). For this example, the building cost C is expressed simply as the sum of a construction (or fabrication) cost C_{con} and a material cost:

$$C = C_{con} + c_s \, V \tag{15}$$

where c_s is the material cost per unit steel volume and V is the volume of steel used in the design. The variation in the construction costs for structural members of different sizes is assumed negligibly small, so that C_{con} is essentially independent of $\boldsymbol{\theta}$. The preference function can then be expressed in terms of a normalized performance parameter:

$$q_{cost} = (C - C_{min}) \,/\, (C_{max} - C_{min}) = (V - V_{min}) \,/\, (V_{max} - V_{min}) \tag{16}$$

where V_{max}=22140 in^3 and V_{min}=4500 in^3 are the steel volumes corresponding to the maximum and minimum allowable member section sizes prescribed by the geometric constraints. The preference function for the building cost can therefore be expressed in terms of the steel volume $V(\boldsymbol{\theta})$ for a design given by $\boldsymbol{\theta}$. As shown in Figure 11(c), a linearly decreasing function is used to specify the preference values for the building cost in terms of the steel volume, with $\mu = 1$ at the minimum allowable volume and $\mu = 0$ at the maximum allowable volume. In the tables of results presented later, the building cost is reported as the volume of steel, V.

Three modes of "failure" are considered for the example building in this study. They are related to lifetime interstory drift risk, code-based maximum allowable interstory drift (ICBO 1994), and code-based maximum allowable column and beam stresses (AISC 1989). The corresponding preference functions are shown in Figure 11(d), (e) and (f), respectively. The code-based maximum allowable interstory drift is calculated using the UBC (ICBO 1994) design response spectrum and employing standard modal analysis and combination methods. As it can be seen from Figure 11(e), a computed interstory drift ratio lower than 2.7% is considered perfectly acceptable, while one higher than 3% is considered completely unacceptable. In Figure 11(f), the preference functions for maximum allowable column and beam normalized stresses are given. The performance parameter σ in this figure is the ratio of the maximum induced stress to the allowable stress specified in the AISC Manual of Steel Construction (AISC 1989). Resulting stresses less than 90% of the code-allowables are considered perfectly acceptable while those greater than the code-allowables are considered completely unacceptable.

The difference between lifetime interstory drift risk and code-based interstory drift is that the former one gives the failure probability of the structure by considering the uncertainties in future loadings using a site-specific seismic environment explicitly, while the code-based calculations consider the deterministic design response spectrum specified in the code. The explicit consideration of the failure probability is of great importance in the design process since it provides flexibility in specifying preferences on the reliability of the structure. However, the code-based requirements can be explicitly included in the design criteria to ensure that the legal requirements are satisfied by the optimal design.

Unacceptable drift performance or "failure" occurs if the maximum interstory drift ratio $d_{\max}$ exceeds a specified allowable drift ratio $d_{allow} = 3\%$ over the lifetime of the structure. The performance parameter is taken as the interstory drift risk, F_d, which is simply equal to the probability of exceeding d_{allow} over the lifetime of the structure. As shown in Figure 11(d), the interstory drift risk F_d is required to be less than a limit value F_u, with greatest preference $\mu = 1$ given to risks (failure probabilities) which are less than a value F_l. In the numerical results, two cases are considered in order to examine their effects on the optimal design: $F_l = 5\%$, $F_u = 10\%$ (the 5% risk case) and $F_l = 1\%$, $F_u = 2\%$ (the 1% risk case). The risk F_d is computed using a probabilistic seismic hazard model and probabilistic structural analysis tools. For simplicity, linear dynamics are used to approximately compute the deformations even though for large drifts the structural response would involve inelastic behavior.

The code criteria, when included, are based on the Uniform Building Code requirements (ICBO 1994), for seismic zone factor Z=0.4, soil type S=2, importance factor I=1.0 and reduction factor R_w=12. The requirements on the maximum column and beam stresses are computed under the reduced (by R_w) code forces. The maximum interstory drift ratio d_{code} must be less than 3% under forces specified by the code response spectrum with no reduction by R_w.

6.2 Probabilistic Seismic Hazard Model

In the probabilistic structural analysis considered here, a response spectrum approach is used to compute the response quantities of interest. The ground motion is characterized by the pseudo-velocity response spectrum $S_{\rm V}(T,\ \zeta)$ where T is the period and ζ is the critical damping ratio of a single degree-of-freedom linear oscillator. The attenuation formula proposed by Boore et al. (1993) is used to model $S_{\rm V}(T,\ \zeta)$ in terms of earthquake magnitude and epicentral distance.

The attenuation relationship is given as

$$log_{10}(S_{\rm V}(T,\ \zeta)) = log_{10}(\widehat{S}_{\rm V}(T,\ \zeta)) + \varepsilon(T,\ \zeta) \tag{17}$$

where

$$\begin{aligned} log_{10}(\widehat{S}_{\rm V}(T,\ \zeta)) \ &= \ \widehat{b}_1 + \widehat{b}_2\ (M-6) + \widehat{b}_3\ (M-6)^2 + \widehat{b}_4\ r + \\ &\quad \widehat{b}_5\ log(r) + \widehat{b}_6\ G_b + \widehat{b}_7\ G_c \end{aligned} \tag{18}$$

Here $r = \sqrt{R^2 + h^2}$, where R is the epicentral distance and h is a fictitious event depth determined by the regression analysis; G_b and G_c are soil type parameters which take a value 0 or 1 depending on the soil classification at the site. The best estimates of the parameters $\widehat{b}_i \equiv \widehat{b}_i(T,\ \zeta)$ appearing in the model for $\widehat{S}_{\rm V}(T,\ \zeta)$ have been determined by Boore et al. (1993, 1994) by regression analysis of a large database of accelerograms for four different damping values (ζ = 2%, 5%, 10% and 20%) and 46 different period values ranging from 0.1 to 2.0s and cubic spline fits are obtained for each parameter as a function of the period and the critical damping ratio. For a complete description of all variables appearing in the attenuation formula (18), the reader is referred to Boore et al. (1993, 1994).

The function $\varepsilon(T,\ \zeta)$ in (17) represents the uncertain model error in the actual spectral amplitudes $S_{\mathrm{V}}(T,\ \zeta)$ compared with the estimated amplitudes $\widehat{S}_{\mathrm{V}}(T,\ \zeta)$ from the model. The probability density function for $\varepsilon(T,\ \zeta)$ is assumed to follow a Gaussian distribution over the range of periods analyzed, with zero mean and variance given in Boore et al. (1994).

In this study, only the epicentral distance R and the earthquake magnitude M are considered as the uncertain "seismicity" variables. The probability distribution for these parameters is derived by assuming a simple seismicity model as follows. The earthquake sources are point sources located in a circular area with a radius of $R_{\max}$ centered at the site where the building is located. It is assumed that an earthquake is equally likely to occur at any point inside this circular source region, so the probability $p(R)dR$ is simply the ratio of the area of a strip of width dR located R distance away from the center to the area of the circle with radius $R_{\max}$, yielding the probability density function:

$$p(R) = 2R\ /\ R_{\max}^2 \tag{19}$$

The probability density function $p(M)$ for the earthquake magnitude is based on a truncated Gutenberg-Richter relationship (Gutenberg and Richter 1958):

$$p(M) = b'\ e^{-b'M}/(e^{-b'M_{\min}} - e^{-b'M_{\max}}) \tag{20}$$

where $M_{\min}$ and $M_{\max}$ are the regional lower and upper bounds for the earthquake magnitude, and $b' = b\ \log_e(10)$. The expected number of events per annum falling into the magnitude range considered is $\nu = 10^{a-bM_{\min}} - 10^{a-bM_{\max}}$. The following data are used for the parameters of the seismicity model: $R_{\max} = 50$ km, $M_{\min} = 5.0$, $M_{\max} = 7.7$, $b = 1.0$ and a is chosen to give a desired value of ν, the seismicity rate. It is assumed that the surrounding seismic region is not capable of generating earthquakes with magnitudes greater than 7.7, and that earthquakes with magnitudes less than 5.0 have no structural design consequences. To give a qualitative illustration of the seismic environment considered, the pseudo-velocity response spectrum specified by UBC (ICBO 1994) for the example building structure is compared, in Figure 12, with pseudo-velocity response spectra for various exceedence probability levels. These uniform hazard spectra were obtained from the attenuation formula given by Boore et al. (1993) for the seismic environment described above, with $a = 5.0$, which corresponds to a seismicity rate of 1 event per annum in the magnitude range chosen. Depending on the period range, the UBC spectrum falls between the 4% and 15% exceedence levels of the probabilistic response spectrum.

It should be noted that the epicentral distance and the earthquake magnitude are assumed to be stochastically independent, although a more refined probability could be based on extended earthquake sources and allow correlation between R and M for larger values of M.

6.3 Reliability Computations

The uncertain parameter set $\boldsymbol{\phi}$ for the ground motion model describing $S_{\mathrm{V}}(T,\ \zeta)$ consists of the magnitude M and the epicentral distance R, so the probability density function corresponding to $p(\boldsymbol{\alpha} \mid \boldsymbol{\phi})$ in the general theory described earlier is $p(\mathbf{S}_{\mathrm{V}} \mid M,\ R)$ where

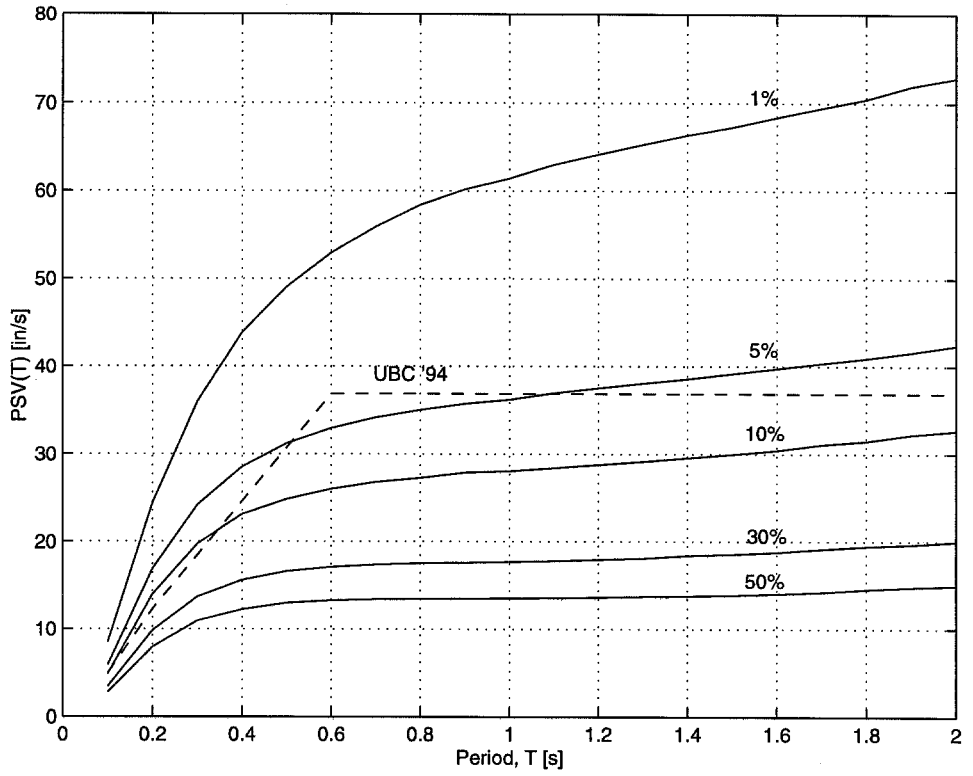

Figure 12: Comparison of UBC (1994) Response Spectrum and the Seismic Hazard Levels for the Chosen Seismicity with $a = 5.0$

$\mathbf{S_V} = [S_V(T_1,\ \zeta_1),\ \ldots,\ S_V(T_n,\ \zeta_n)]^T$ and n is the number of modes contributing significantly to the displacement response. A probability model which assumes stochastic independence of the spectral ordinates is used, so:

$$p(\mathbf{S_V} \mid M,\ R) = \prod_{j=1}^{n} p(S_V(T_j,\ \zeta_j) \mid M,\ R) \tag{21}$$

where each probability density function in the product is a log-normal distribution implied by equation (17).

Since the ground motion is characterized by the pseudo-velocity response spectrum $S_V(T,\ \zeta)$, a response spectrum analysis is used to compute the peak interstory drift d_i of the i-th story. To this end, available modal combination rules may be used to estimate d_i from the maximum effective modal drifts $\xi_{ij} = \beta_{ij}\ S_V(T_j,\ \zeta_j)$ for each mode j (e.g. Der Kiureghian 1981), where T_j is the modal period, ζ_j is the modal damping ratio, and β_{ij} is the corresponding effective modal participation factor for the i-th floor, which depends on the j-th modal properties. These properties are computed through an eigenvalue analysis of the structure corresponding

to a particular $\boldsymbol{\theta}$. Assuming well-separated structural modal frequencies, one obtains

$$d_i = (\beta_{i1}^2 \; S_{\mathrm{V}}^2(T_1, \; \zeta_1) + \; \cdots + \; \beta_{in}^2 \; S_{\mathrm{V}}^2(T_n, \; \zeta_n)^{1/2} \tag{22}$$

Structural modeling errors and the uncertainty in the estimate for d_i given by the modal combination rule are ignored in this example, but these effects could be included.

Assuming that the occurences of earthquake events follow a Poisson arrival process, the drift risk $F_d(\boldsymbol{\theta}, \; t) = P(d_{\max} > d_{allow} \mid \boldsymbol{\theta}, \; t)$ over the lifetime t of the structure is computed from (7), where

$$F(\boldsymbol{\theta}) = P(d_{\max} > d_{allow} \mid \boldsymbol{\theta}) = P(\bigcup_{i=1}^{n} \{d_i > d_{allow}\} \mid \boldsymbol{\theta}) \tag{23}$$

is the failure probability, given the occurrence of an event. Note that $F(\boldsymbol{\theta})$ can be simplified to the form (6), where $\boldsymbol{\alpha} = \mathbf{S}_{\mathrm{V}}$, $\boldsymbol{\phi} = (M, \; R)$ and $F(\boldsymbol{\theta} \mid \boldsymbol{\alpha}) = P(d_{\max} > d_{allow} \mid \mathbf{S}_{\mathrm{V}}, \; \boldsymbol{\theta})$. Under the previous assumption that the interstory drifts are known once $\mathbf{S}_{\mathrm{V}}$ and $\boldsymbol{\theta}$ are given, it is clear that the resulting conditional failure probability $P(d_{\max} > d_{allow} \mid \mathbf{S}_{\mathrm{V}}, \; \boldsymbol{\theta})$ is either 1 or 0, depending on whether the safety levels have been exceeded or not, so the failure probability is given by (14) where $g_i = g_i(\mathbf{S}_{\mathrm{V}}, \; \boldsymbol{\theta}) = d_{allow} - d_i(\mathbf{S}_{\mathrm{V}}, \; \boldsymbol{\theta})$. Integral (14) is in the form of the classical system reliability problem for a series of components in which if any of the components fails, that is, if any $d_i(\mathbf{S}_{\mathrm{V}}, \; \boldsymbol{\theta}) > d_{allow}$, the system is considered failed. The component failure probability, $F_i(\boldsymbol{\theta})$, given an occurence of an event, is given by (10) and is approximated by the asymptotic formula given in (13) where, for this case, $\varphi = S_{\mathrm{V}}(T_1, \; \zeta_1)$ is independent of $\boldsymbol{\psi} = (S_{\mathrm{V}}(T_2, \; \zeta_2), \; \ldots \; , \; S_{\mathrm{V}}(T_n, \; \zeta_n), \; M, \; R)$, and

$$h(\boldsymbol{\psi}) = [d_{allow}^2 - \beta_{i2}^2 \; S_{\mathrm{V}}^2(T_2, \; \zeta_2) - \; \cdots - \; \beta_{in}^2 \; S_{\mathrm{V}}^2(T_n, \; \zeta_n)]^{1/2} / \beta_{i1} \tag{24}$$

The form of $h(\boldsymbol{\psi})$ in (24) is readily derived using $g_i(\mathbf{S}_{\mathrm{V}}, \; \boldsymbol{\theta}) = d_{allow} - d_i(\mathbf{S}_{\mathrm{V}}, \; \boldsymbol{\theta}) = 0$, where d_i is given by (22) and $\varphi = h(\boldsymbol{\psi}) = S_{\mathrm{V}}(T_1, \; \zeta_1)$.

In the numerical results that follow, it will be demonstrated that considering only one failure surface corresponding to the highest component failure probability results in a good approximation of the system reliability for the type of design problem discussed herein.

6.4 Numerical Results

For the numerical study, the modal damping ratios are chosen to be $\zeta_i = 0.05$ for all contributing modes. A lifetime of $t = 50$ years is considered. The results in Table 1 correspond to a seismicity rate $\nu = 1$ event per annum and the case where beams and columns have the same cross-sectional dimensions, that is, $B_{beam} = B_{col} = B$, $D_{beam} = D_{col} = D$, and so $\boldsymbol{\theta} = (B, \; D)$. Results are shown for both the 5% and 1% risk cases described earlier. As expected, the optimal design for 1% drift risk gives larger member sizes than the 5% risk case does. The code-based based drift and strength requirements (ICBO 1994, AISC 1989) are not included as design criteria for the results in Table 1 since it has been found that failure modes related to them do not control the design of the present structure.

Table 1: Optimal Design for $\nu = 1$ event/yr; Case $\boldsymbol{\theta} = (B,\ D)$

	Continuous Optimization								Genetic Algorithm	
5% Risk										
	1-mode (num)		1-mode (asym)		2-mode (asym)		3-mode (asym)		1-mode (num)	
Criteria	Value	μ	Value	μ	Value	μ	Value	μ	Value	μ
B	4.10	1.0000	4.10	1.0000	4.10	1.0000	4.10	1.0000	W8x18	1.0000
D	9.74	1.0000	8.71	1.0000	8.71	1.0000	8.71	1.0000		1.0000
Vol	6277	0.8992	5906	0.9203	5907	0.9202	5909	0.9201	7467	0.8318
$F_{d,1}$	0.0163	-	0.0214	-	0.0220	-	0.0220	-	0.0171	-
$F_{d,2}$	0.0500	-	0.0500	-	0.0500	-	0.0500	-	0.0522	-
$F_{d,3}$	0.0179	-	0.0228	-	0.0247	-	0.0247	-	0.0187	-
F_d	0.0500	1.0000	0.0500	1.0000	0.0500	1.0000	0.0500	1.0000	0.0522	0.9568
Overall		**0.9738**		**0.9794**		**0.9794**		**0.9794**		**0.9445**
Period	T_1=1.106 s		T_1=1.260 s		T_1=1.260 s		T_1=1.258 s		T_1=1.121 s	
1% Risk										
	1-mode (num)		1-mode(asym)		2-mode (asym)		3-mode (asym)		1-mode (num)	
Criteria	Value	μ	Value	μ	Value	μ	Value	μ	Value	μ
B	4.10	1.0000	4.10	1.0000	4.10	1.0000	4.10	1.0000	W14x22	1.0000
D	13.99	1.0000	13.67	1.0000	13.67	1.0000	13.67	1.0000		1.0000
Vol	7807	0.8125	7692	0.8190	7693	0.8190	7694	0.8189	9153	0.7364
$F_{d,1}$	0.0025	-	0.0034	-	0.0035	-	0.0035	-	0.0011	-
$F_{d,2}$	0.0100	-	0.0100	-	0.0100	-	0.0100	-	0.0052	-
$F_{d,3}$	0.0029	-	0.0038	-	0.0039	-	0.0039	-	0.0052	-
F_d	0.0100	1.0000	0.0100	1.0000	0.0100	1.0000	0.0100	1.0000	0.0052	1.0000
Overall		**0.9494**		**0.9513**		**0.9513**		**0.9513**		**0.9263**
Period	T_1=0.722 s		T_1=0.742 s		T_1=0.742 s		T_1=0.742 s		T_1=0.632 s	

The results for one, two and three contributing structural modes are obtained using the asymptotic approximation of the failure probability integral (Papadimitriou, Beck, and Katafygiotis 1997). In the case of one structural mode, a numerical integration scheme is also used to provide an accuracy check for the more efficiently calculated asymptotic results. It is observed from Table 1 that the asymptotic approximation gives results similar to those obtained from numerical integration, especially for higher reliability requirements. Also, it can be seen that the second and third translational modes do not have a significant effect on the optimal design of the three-story structure considered in this study.

Note that in Table 1, and in other cases shown below, the optimal flange width B is always 4.10 in, which corresponds to the lower corner of the preference function for B shown in Figure 11(a). This occurs because it is more cost-effective to provide the necessary bending stiffness by increasing the web depth D rather than the flange width B. However, if B is reduced below 4.10 in, the rate of reduction in the preference in Figure 11(a) outweighs the improvement in the cost preference in Figure 11(c).

In Table 1, $F_{d,i}$, i=1,2,3, denote the drift risk for the i-th story over the lifetime t of the structure. It was found that the interstory drift risk $F_{d,2}$ for the second story governs the design for the example problem at hand. This is because of the rotational constraints at the base of the first story columns. Specifically, it was found that the failure regions defined by the failure surfaces $g_1(\mathbf{S_V}) = 0$ and $g_3(\mathbf{S_V}) = 0$ for the first and third stories, respectively, are subsets of the failure region defined by the dominant failure surface $g_2(\mathbf{S_V}) = 0$ in the region of high probability. This can be seen from Figure 13 which gives the composite plot of the failure surfaces $g_1(\mathbf{S_V}) = 0$, $g_2(\mathbf{S_V}) = 0$, $g_3(\mathbf{S_V}) = 0$ in the space of the pseudo-velocity responses of the first and second modes of the structure, and the contour plots of the respective probabilities $p(\mathbf{S_V})$ of observing those pseudo-velocities for the given seismic environment model. The probability density function for $\mathbf{S_V}$ shown in Figure 13 is given by

$$p(\mathbf{S_V}) = \int_M \int_R p(\mathbf{S_V} \mid M,\ R)\ p(M)\ p(R)\ dR\ dM \tag{25}$$

where the integration is carried out numerically. From the demonstration in Figure 13 it is clear that the contributions in equation (14) to the system failure probability F_d from the failure surfaces $g_1(\mathbf{S_V}) = 0$ and $g_3(\mathbf{S_V}) = 0$ for the first and third story drifts are negligible.

In Table 2, the case of four design parameters, $\boldsymbol{\theta} = (B_{beam},\ D_{beam},\ B_{col},\ D_{col})$, is presented which allows beam and column cross-sectional dimensions to be different but all beams must have the same cross-section and so do all columns. Comparing the building costs (steel volumes) in Tables 1 and 2, it is observed that by treating the sizes of beams and columns independently, the optimal designs are slightly less costly, as expected. However, in both cases, the dynamics of the resulting optimal structures are similar as illustrated by the similar fundamental periods in Tables 1 and 2.

The optimal design applying the vGA genetic algorithm to a discrete optimization over a set of 128 of the more relevant AISC W-shape steel sections is also presented in the last column of Tables 1 and 2. An increase in building cost (corresponding to 20% or so increase in steel volume) occurs compared with the continuous optimization case. This is due to the limited variety of steel-section sizes in the discrete case.

Table 2: Optimal Design for $\nu = 1$ event/yr; Case $\boldsymbol{\theta} = (B_{beam},\ D_{beam},\ B_{col},\ D_{col})$

	Continuous Optimization								Genetic Algorithm	
5% Risk										
	1-mode (num)		1-mode (asym)		2-mode (asym)		3-mode (asym)		1-mode (num)	
Criteria	Value	μ	Value	μ	Value	μ	Value	μ	Value	μ
B_{beam}	4.10	1.0000	4.10	1.0000	4.10	1.0000	4.10	1.0000	W8x18	1.0000
D_{beam}	11.00	1.0000	9.80	1.0000	9.79	1.0000	9.76	1.0000		1.0000
B_{col}	4.10	1.0000	4.10	1.0000	4.10	1.0000	4.10	1.0000	W8x18	1.0000
D_{col}	8.11	1.0000	7.33	1.0000	7.34	1.0000	7.40	1.0000		1.0000
Vol	6211	0.9030	5854	0.9232	5856	0.9231	5860	0.9229	7467	0.8318
$F_{d,1}$	0.0252	-	0.0291	-	0.0298	-	0.0294	-	0.0171	-
$F_{d,2}$	0.0500	-	0.0500	-	0.0500	-	0.0500	-	0.0522	-
$F_{d,3}$	0.0129	-	0.0182	-	0.0200	-	0.0201	-	0.0187	-
F_d	0.0500	1.0000	0.0500	1.0000	0.0500	1.0000	0.0500	1.0000	0.0522	0.9568
Overall		**0.9831**		**0.9868**		**0.9868**		**0.9867**		**0.9627**
Period	T_1=1.128 s		T_1=1.121 s		T_1=1.278 s		T_1=1.276 s		T_1=1.121 s	
1% Risk										
	1-mode (num)		1-mode(asym)		2-mode (asym)		3-mode (asym)		1-mode (num)	
Criteria	Value	μ	Value	μ	Value	μ	Value	μ	Value	μ
B_{beam}	4.10	1.0000	4.10	1.0000	4.10	1.0000	4.10	1.0000	W14x22	1.0000
D_{beam}	15.75	1.0000	15.38	1.0000	15.37	1.0000	15.35	1.0000		1.0000
B_{col}	4.10	1.0000	4.10	1.0000	4.10	1.0000	4.10	1.0000	W14x22	1.0000
D_{col}	11.76	1.0000	11.50	1.0000	11.51	1.0000	11.54	1.0000		1.0000
Vol	7725	0.8172	7610	0.8237	7611	0.8236	7612	0.8236	9153	0.7362
$F_{d,1}$	0.0042	-	0.0051	-	0.0051	-	0.0051	-	0.0011	-
$F_{d,2}$	0.0100	-	0.0100	-	0.0100	-	0.0100	-	0.0052	-
$F_{d,3}$	0.0020	-	0.0029	-	0.0030	-	0.0030	-	0.0013	-
F_d	0.0100	1.0000	0.0100	1.0000	0.0100	1.0000	0.0100	1.0000	0.0052	1.0000
Overall		**0.9669**		**0.9682**		**0.9682**		**0.9682**		**0.9502**
Period	T_1=0.734 s		T_1=0.755 s		T_1=0.755 s		T_1=0.754 s		T_1=0.632 s	

Table 3: Optimal Design for $\nu = 0.5,\ 1,\ 2$ events/yr; Case $\boldsymbol{\theta} = (B_{beam},\ D_{beam},\ B_{col},\ D_{col})$

5% Risk with 1-mode numerical integration						
	$\nu = 0.5$		$\nu = 1$		$\nu = 2$	
Criteria	Value	μ	Value	μ	Value	μ
B_{beam}	4.10	1.0000	4.10	1.0000	4.10	1.0000
D_{beam}	9.15	1.0000	11.00	1.0000	13.00	1.0000
B_{col}	4.10	1.0000	4.10	1.0000	4.10	1.0000
D_{col}	6.75	1.0000	8.11	1.0000	9.63	1.0000
Vol	5634	0.9357	6211	0.9030	6845	0.8670
σ^b_{max}	0.1947	1.0000	0.1521	1.0000	0.1423	1.0000
σ^c_{max}	0.6312	1.0000	0.5467	1.0000	0.5057	1.0000
d_{code}	0.0246	1.0000	0.0161	1.0000	0.0128	1.0000
$F_{d,1}$	0.0263	-	0.0252	-	0.0238	-
$F_{d,2}$	0.0500	-	0.0500	-	0.0500	-
$F_{d,3}$	0.0140	-	0.0129	-	0.0119	-
F_d	0.0500	1.0000	0.0500	1.0000	0.0500	1.0000
Overall		**0.9926**		**0.9887**		**0.9843**
Period	T_1=1.396 s		T_1=1.128 s		T_1=0.926 s	

1% Risk with 1-mode numerical integration						
	$\nu = 0.5$		$\nu = 1$		$\nu = 2$	
Criteria	Value	μ	Value	μ	Value	μ
B_{beam}	4.10	1.0000	4.10	1.0000	4.10	1.0000
D_{beam}	13.75	1.0000	15.75	1.0000	17.58	1.0000
B_{col}	4.10	1.0000	4.10	1.0000	4.10	1.0000
D_{col}	10.15	1.0000	11.76	1.0000	13.39	1.0000
Vol	7075	0.8540	7725	0.8172	8346	0.7820
σ^b_{max}	0.1405	1.0000	0.1364	1.0000	0.1333	1.0000
σ^c_{max}	0.4955	1.0000	0.4660	1.0000	0.4400	1.0000
d_{code}	0.0120	1.0000	0.0101	1.0000	0.0088	1.0000
$F_{d,1}$	0.0046	-	0.0042	-	0.0037	-
$F_{d,2}$	0.0100	-	0.0100	-	0.0100	-
$F_{d,3}$	0.0022	-	0.0020	-	0.0017	-
F_d	0.0100	1.0000	0.0100	1.0000	0.0100	1.0000
Overall		**0.9826**		**0.9778**		**0.9730**
Period	T_1=0.868 s		T_1=0.734 s		T_1=0.637 s	

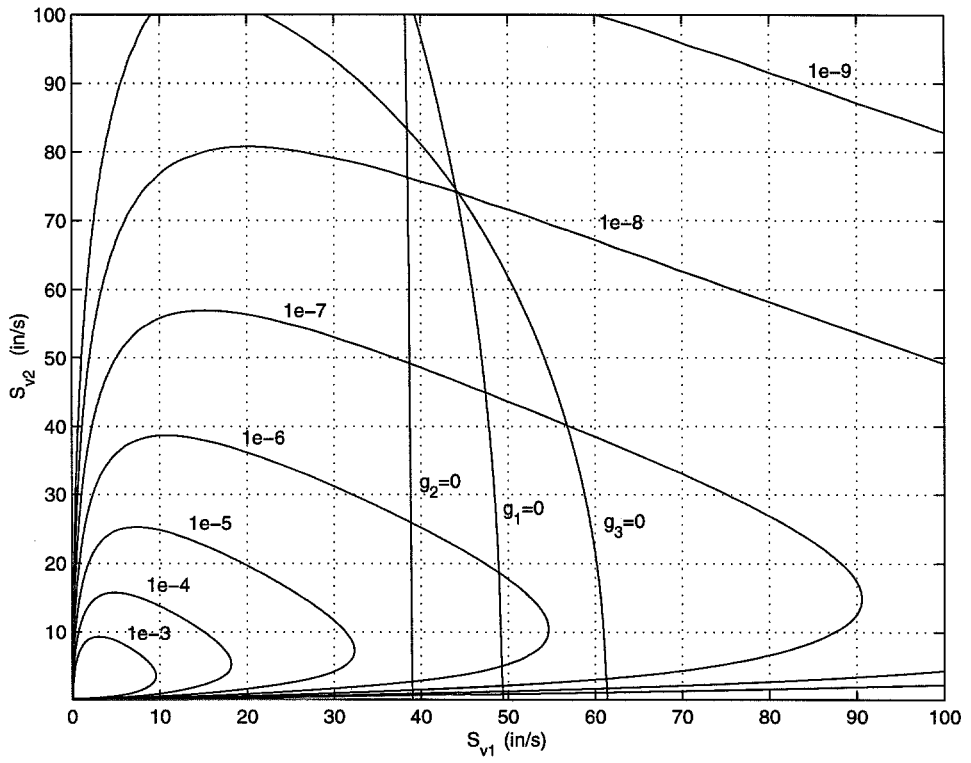

Figure 13: Interstory Drift Failure Surfaces for 5% Risk, and $p(S_{\mathrm{v1}},\ S_{\mathrm{v2}})$ Contours

In Table 3, the effect of the regional seismicity rate on the optimal design is investigated. Results are presented for the three seismicity rates corresponding to $\nu = 0.5$, 1 and 2 events per annum and for 5% and 1% drift risk cases. As expected, higher seismicity or lower risk requirements lead to larger structural members. Note that the UBC requirements reflected in Figure 11(e) and (f) are also included as design criteria. The dynamic lateral-load calculation procedure for the code-based performance parameters, that is, maximum column stress, maximum beam stress and maximum interstory drift, in Table 3 is based on the response spectra described in the 1994 UBC (ICBO 1994). For all six cases presented in Table 3, the drift reliability requirement is found to be more stringent than what the UBC demands, so the UBC requirements have no influence on the final design. This can be seen from the fact that the code stress ratios for the beams and columns, σ^b_{max} and σ^c_{max} respectively, are less than 0.9 and the code interstory drift d_{code} is lower than 2.7%, so from the code point-of-view, they provide a fully satisfactory design (see Figure 11(e) and (f)). One can conclude from this fact that even for the lowest seismicity specified in Table 3, the lifetime interstory drift reliability is less than 95% for a purely code-based optimal design.

In Table 4, the effect on reliability-based optimal designs of increasing the importance weight, w_{Vol}, for the building cost criterion is illustrated for the 5% and 1% risk cases. At first, as w_{Vol} increases from 1 to 10, the drift risk F_d=5% (or F_d=1%) continues to control

Table 4: Optimal Design for $\nu = 1$ event/yr; Case $\boldsymbol{\theta} = (B,\ D)$

5% Risk with 1-mode numerical integration								
	w_{Vol}=1		w_{Vol}=10		w_{Vol}=50		w_{Vol}=100	
Criteria	Value	μ	Value	μ	Value	μ	Value	μ
B	4.10	1.0000	4.10	1.0000	4.10	1.0000	4.10	1.0000
D	9.74	1.0000	9.74	1.0000	8.79	1.0000	8.45	1.0000
Vol	6277	0.8992	6277	0.8992	5936	0.9186	5815	0.9255
$F_{d,1}$	0.0163	-	0.0163	-	0.0251	-	0.0294	-
$F_{d,2}$	0.0500	-	0.0500	-	0.0730	-	0.0840	-
$F_{d,3}$	0.0179	-	0.0179	-	0.0273	-	0.0319	-
F_d	0.0500	1.0000	0.0500	1.0000	0.0730	0.5394	0.0840	0.3195
Overall		**0.9738**		**0.9216**		**0.9123**		**0.9174**
Period	T_1=1.106 s		T_1=1.106 s		T_1=1.246 s		T_1=1.304 s	

1% Risk with 1-mode numerical integration								
	w_{Vol}=1		w_{Vol}=10		w_{Vol}=50		w_{Vol}=100	
Criteria	Value	μ	Value	μ	Value	μ	Value	μ
B	4.10	1.0000	4.10	1.0000	4.10	1.0000	4.10	1.0000
D	13.99	1.0000	13.99	1.0000	12.87	1.0000	12.54	1.0000
Vol	7807	0.8125	7807	0.8125	7406	0.8353	7286	0.8421
$F_{d,1}$	0.0025	-	0.0025	-	0.0042	-	0.0048	-
$F_{d,2}$	0.0100	-	0.0100	-	0.0153	-	0.0173	-
$F_{d,3}$	0.0029	-	0.0029	-	0.0047	-	0.0055	-
F_d	0.0100	1.0000	0.0100	1.0000	0.0153	0.4710	0.0173	0.2679
Overall		**0.9494**		**0.8524**		**0.8319**		**0.8355**
Period	T_1=0.722 s		T_1=0.722 s		T_1=0.797 s		T_1=0.822 s	

the optimal design, which therefore does not change. When w_{Vol}=50 (or 100), however, the cost criterion is influential in the trade-off and so a more "aggressive" design with lower cost (or steel volume) but higher risk, F_d, is produced.

7 EXAMPLE II

To demonstrate the application of the methodology to performance-based design and how it can be utilized in other ways, the same structure considered in Example I is designed using the performance levels given in *Vision 2000* (SEAOC 1995). The same uncertain seismic environment and probabilistic structural analysis based on the response spectrum approach are used in estimating the performance of the structure during its lifetime. The epicentral distance R and the earthquake magnitude M are treated as the only uncertain seismicity parameters. The source region regarding the distribution of R is same as in Example I, that is, an earthquake is equally likely to occur at any point inside a circular source region centered at the site where the building is located and with a radius $R_{\max} = 50$ km. For the distribution of the earthquake magnitudes, M, the truncated Gutenberg-Richter relationship (20) is used

Table 5: Performance Levels of *Vision 2000* (SEAOC 1995)

Performance Level	*Description*
Fully Operational (0.2%)	No significant damage in structural and non-structural components. The building can be occupied and is available for its intended use.
Operational (0.5%)	Light damage in structural elements. Moderate damage in non-structural elements. The building can be occupied for its intended use but some functions may be disrupted
Life-Safe (1.5%)	Moderate damage in structural and non-structural elements. Loss in lateral stiffness and reduced ability to resist additional lateral loads. The building cannot be occupied, but may be repaired.
Near Collapse (2.5%)	Extreme damage state. The building cannot be occupied, and it is unlikely to be repaired.

with the same parameters $M_{min} = 5.0$, $M_{max} = 7.7$, $b = 1.0$ and $a = 5.0$ as before, implying a seismicity rate of $\nu = 1$ event per annum in the magnitude range of interest.

7.1 Performance-Based Design - *Vision 2000*

In performance-based structural design, one tries to design a structure to satisfy multiple performance levels under various excitations it might experience during its lifetime. Actually, this design concept is at the heart of all structural design, but until very recent times, the various performance levels were not quantitatively specified and were not explicitly taken into consideration. Due to the unsatisfactory performances of engineered structures during recent earthquakes, the demand for multi-level performance-based design is causing dramatic changes in the way structures are designed.

Vision 2000, published by Structural Engineers Association of California in 1995, includes a collection of suggested qualitative performance levels as well as quantified levels for some performance criteria. For the application of the multi-criteria performance-based optimal structural design methodology explained in this report, the *Vision 2000* performance levels on the interstory drift ratios are used.

In *Vision 2000*, the expected performance levels for different earthquake design levels vary with the importance of the structure. In the example below, the structure is assumed to follow the "basic objective" requirements of the *Vision 2000*: to be "fully operational" after "frequent" earthquakes; to be "operational" after "occasional" earthquakes; to be "life-safe" after "rare" earthquakes; and to be "near collapse" after "very rare" earthquakes. The descriptions of the four performance levels together with corresponding interstory drift ratios, and the four earthquake design levels are given in Tables 5 and 6, respectively. In Table 6, the earthquake design level exceedance probabilities normalized for the lifetime of 50 years of the example structure are also given. This normalization can be made using the given recurrence intervals,

Table 6: Earthquake Design Levels of *Vision 2000* (SEAOC 1995)

Earthquake Design Level	*Recurr. Interval*	*Prob. of Exceed.*	*Prob. of Exceed. in* t_{life}
Frequent	43 years	50% in 30 years	68.5% in 50 years
Occasional	72 years	50% in 50 years	50% in 50 years
Rare	475 years	10% in 50 years	10% in 50 years
Very Rare	970 years	10% in 100 years	5.13% in 50 years

together with the assumption that the earthquake occurences follow a Poisson arrival process as implied in *Vision 2000.*

It should be noted that, in *Vision 2000*, the reliabilities, or the exceedance probabilities, are given on the earthquake design level rather than on the performance level. It seems more appropriate to the philosophy of performance-based design to specify the reliabilities (or the failure probabilities) on the performance levels since one has no control on the seismic environment, and the concept of performance-based design is based on meeting various levels of "expected" performance of the structure. For example, it is desirable to keep the specified performance levels for similar structures (e.g. structures needed during emergency response) to be the same no matter what the seismic environment is. It is better to focus on directly controlling the seismic risk rather than trying to control it by specifying seismic hazard levels. Notwithstanding this conceptual difference, specifying the reliabilites on seismic hazard levels, as implied in *Vision 2000*, and specifying the reliabilities on seismic risk levels, as done in the methodology presented in this report, yield equivalent results when a linear single-mode analysis is considered during the design of a structure. However, further investigation of the effects of the two design philosophies is desirable.

7.2 Numerical Results

In the second example, for the performance levels in Table 5, the following interstory drift ratio and corresponding failure probability (exceedance probability, or risk) over the lifetime t=50 years, are used: 0.2% with 68.5% risk, 0.5% with 50% risk, 1.5% with 10% risk, and 2.5% with 5.13% risk. These risk levels correspond to F_l in Figure 11(d) (while $F_u = 1.01F_l$ is chosen). The chosen design parameters are the member flange width B and web depth D for the beams and columns, that is, $\boldsymbol{\theta} = (B_{beam},\ D_{beam},\ B_{col},\ D_{col})$. As before, the flange and web plate thicknesses are held fixed at 0.25 inches. Continuous optimization over the dimension ranges shown in Figure 11 is performed and, as in Example I, the adaptive random search algorithm is employed during the search for optimal design. The 1994 UBC requirements on interstory drift ratios and maximum beam and column stresses are also considered in this example to show that these code criteria do not control the optimal design. The same dead load and live load values as in Example I are considered for computing the gravity loads.

In Table 7, the resulting optimum designs for each of the four performance levels are given. It should be noted that, in order to be able to see the effect on the optimal design of each performance level, the levels are considered one at a time. As stated earlier, the interstory

Table 7: Optimal Design for $\nu = 1$ event/yr; Case $\boldsymbol{\theta} = (B_{beam},\ D_{beam},\ B_{col},\ D_{col})$

1-mode numerical integration								
	Freq./Fully Oper.		Occas./Oper.		Rare/Life-Safe		V. Rare/Coll.(2.5%)	
Criteria	Value	μ	Value	μ	Value	μ	Value	μ
B_{beam}	4.10	1.0000	4.10	1.0000	4.10	1.0000	4.10	1.0000
D_{beam}	29.90	1.0000	20.51	1.0000	15.28	1.0000	12.47	1.0000
B_{col}	4.10	1.0000	4.10	1.0000	4.10	1.0000	4.10	1.0000
D_{col}	26.54	1.0000	15.22	1.0000	11.19	1.0000	9.21	1.0000
Vol	12932	0.5220	9203	0.7334	7537	0.8279	6674	0.8768
σ^b_{max}	0.0585	1.0000	0.1140	1.0000	0.1369	1.0000	0.1435	1.0000
σ^c_{max}	0.2381	1.0000	0.3990	1.0000	0.4767	1.0000	0.5147	1.0000
d_{code}	0.0022	1.0000	0.0066	1.0000	0.0106	1.0000	0.0134	1.0000
$F_{d,1}$	0.3551	-	0.3039	-	0.0514	-	0.0255	-
$F_{d,2}$	0.6850	-	0.5000	-	0.1000	-	0.0513	-
$F_{d,3}$	0.3420	-	0.1876	-	0.0266	-	0.0131	-
F_d	0.6850	1.0000	0.5000	1.0000	0.1000	1.0000	0.0513	1.0000
Overall		**0.9303**		**0.9661**		**0.9792**		**0.9855**
Period	T_1=0.305 s		T_1=0.537 s		T_1=0.770 s		T_1=0.974 s	

Table 8: Reliabilities for the Four Performance Levels for Four Optimal Designs

Design \ Analysis	Fully Oper.	Operational	Life-Safe	Near Coll.
Frequent—Fully Oper. (0.2%, 31.5%)	**0.3150**	0.9373	0.9996	1.0000
Occasional—Operational (0.5%, 50%)	0.0047	**0.5000**	0.9748	0.9963
Rare—Life-Safe (1.5%, 90%)	0.0008	0.1872	**0.9000**	0.9780
Very Rare—Near Coll. (2.5%, 94.87%)	0.0000	0.0696	0.8049	**0.9487**

drift risk is the chosen reliability-based performance parameter.

In Table 8, the reliabilities corresponding to different performance levels for each of the four optimal designs are compared. For example, in the first row, results for the optimal design for "fully operational after a frequent event" are presented, showing that for this design, the reliabilities for the other three performance levels are exceedingly high, that is, the corresponding performance objectives are met by a very high margin. Table 8 also shows that an optimal design that is based on the criterion of being "operational after an occasional event" does not meet the "fully operational after a frequent event" criterion. Similarly, using "life-safe after a rare event" for the optimal design does not meet the "fully operational after a frequent event" and the "operational after an occasional event" criteria. An optimal design which is based on the "near collapse after a very rare event" objective does not meet any of the other objectives.

A clearer comparison of the interstory drift reliabilities for each of the four optimal designs can be seen in Figure 14. It should be noted that in order to obtain this plot, the reliabilites for each of the optimal designs are calculated for a multitude of finely separated interstory drift ratios. The *Vision 2000* levels appear as merely four points in this plot (shown as squares).

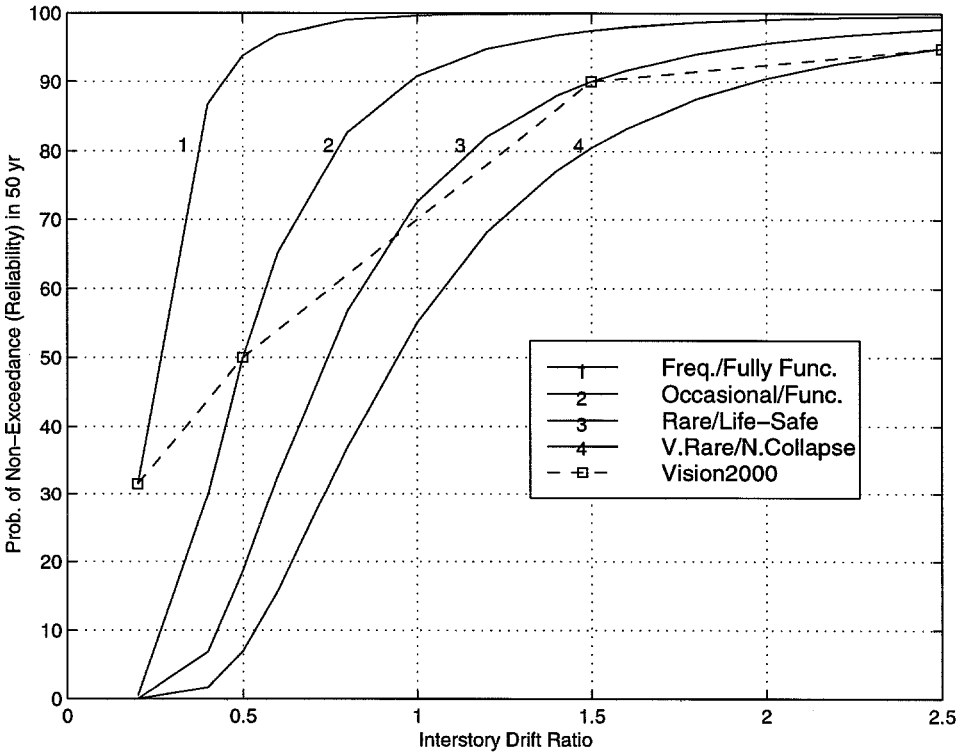

Figure 14: Comparison of Reliabilities for Four Optimal Designs

These four points are connected with dashed straight lines to aid in visual comparison; the resulting reliability curve is artificial, and is neither suggested nor implied in the *Vision 2000* recommendations. From both Table 8 and Figure 14, it is clear that if all the interstory drift performance criteria of the *Vision 2000* are simultaneously used, the optimal design of the structure is governed by the 0.2% interstory drift ratio with a corresponding 68.5% risk over the lifetime, that is, the condition of being "fully operational after frequent events". It should be noted, however, that in this simple example, all reliability calculations are based on linear dynamics since a response spectrum approach is used, but for higher performance levels (life-safe and near-collapse states), nonlinear behavior would be expected.

As this simple yet illustrative example demonstrates, the design methodology provides a framework in which optimal multi-criteria designs, including performance-based designs, can be determined. It can also be used to help interpret the implications of various performance criteria suggested for performance-based structural design.

8 CONCLUSIONS

The proposed optimal design methodology provides a rational basis for incorporating seismic load uncertainties in the design process and to make reliability-based optimal design decisions that meet specified multiple criteria, including performance-based structural criteria. Code-based requirements are also easily incorporated into the process. This new framework is therefore well-suited for performance-based design of structures under uncertainty. Although the optimal design framework has been demonstrated for a special class of ground motion and structural models, it is very flexible and more sophisticated models can easily be treated. For example, advances in ground motion attenuation formulas and seismic hazard models can easily be incorporated into the framework. Also, an inelastic finite element program can be included in the ANALYZER along with reliability approximations for non-linear systems to more realistically treat large deformations. The methodology is also readily extended to include loading uncertainties due to wind, as well as structural modeling uncertainties.

The general framework presented here for multi-criteria optimal design under risk is potentially applicable to a wide range of engineering systems, including buildings, bridges, offshore structures, equipment and piping systems. In fact, the basic methodology has wider applicability for multi-criteria decision making under risk, as required in many other engineering disciplines. Besides being applicable in the design of new structures, the methodology can be used to design cost-effective upgrades of existing structures. Moreover, the methodology can be applied to evaluate the overall status of existing structures in a way that also includes client's preferences.

9 ACKNOWLEDGMENTS

This report is based upon work which begun under the CUREe-Kajima Research Program of the California Universities for Research in Earthquake Engineering and continued under grant CMS-9796135 of the National Science Foundation. The initial version of the CODA software package was developed as a team effort by the authors and H.A. Smith, V. Vance and L. Barroso of Stanford University and S.F. Masri and W.M. Xu of University of Southern California.

References

Adeli, H. (1994). *Advances in Design Optimization.* Chapman and Hall.

AISC (1989). *Manual of Steel Construction - ASD.* American Institute of Steel Construction.

Ang, A. H. and C. A. Cornell (1974). Reliability bases of structural safety and design. *Journal of Structural Engineering, ASCE 100*(ST9), 1755–1769.

Ang, A. H., A. Der Kiureghian, F. Filippou, J. Pires, and E. Polak (1996). *Reliability-Based*

Optimal Aseismic Design of Reinforced Concerte Buildings. CUREE-Kajima Phase II Final Resport, California Universities for Research in Earthquake Engineering, Richmond, CA.

Au, S. K., C. Papadimitriou, and J. L. Beck (1998). Treatment of multiple design points in reliability methods. *Proc. Fourth Int. Conference on Stochastic Structural Dynamics.* Notre Dame, Indiana.

Beck, J. L., E. Chan, A. Irfanoglu, S. Masri, W. M. Xu, H. A. Smith, V. Vance, and L. Barroso (1996a). *New Computer Tools for Optimal Design Decisions in the Presence of Seismic Risk.* CUREe-Kajima Phase II Final Report, California Universities for Research in Earthquake Engineering, Richmond, CA.

Beck, J. L., C. Papadimitriou, E. Chan, and A. Irfanoglu (1996b). Reliability-based optimal design decisions in the presence of seismic risk. *Proc. Eleventh World Conference on Earthquake Engineering.* Paper No. 1058. Elsevier Science Ltd.

Boore, D. M., W. B. Joyner, and T. E. Fumal (1993). *Estimation of Response Spectra and Peak Accelerations from Western North American Earthquakes: An Interim Report.* Open-File Report 93-509, USGS, Menlo Park, CA.

Boore, D. M., W. B. Joyner, and T. E. Fumal (1994). *Estimation of Response Spectra and Peak Accelerations from Western North American Earthquakes: An Interim Report Part 2.* Open-File Report 94-127, USGS, Menlo Park, CA.

Breitung, K. (1989). Asymptotic approximations for probability integrals. *Probabilistic Engineering Mechanics 4*(4), 187–190.

Breitung, K. (1991). Probability approximations by log likelihood maximization. *J. Engrg. Mech., ASCE 117*(3), 457–477.

Bucher, C. G. (1988). Adaptive sampling - an iterative fast Monte Carlo procedure. *Structural Safety 5*, 119–126.

Casciati, F. and L. Faravelli (1985). Structural reliability and structural design optimization. In *Proc. Fourth International Conference on Structural Safety and Reliability, Konishi, I., et al. (eds), Vol. III*, pp. 61–70.

Chan, E. (1997). *Optimal Design of Building Structures Using Genetic Algorithms.* Ph. D. thesis, EERL Report No. 97-06, Earthquake Engineering Research Laboratory, California Institute of Technology.

Cherng, R. H. and Y. K. Wen (1994). Reliability of uncertain nonlinear trusses under random excitation II. *J. Engrg. Mech., ASCE 120*(4), 748–757.

Cohon, J. L. (1978). *Multiobjective Programming and Planning.* Academic Press.

Deodatis, G. (1991). Weighted integral method II: Response variability and reliability. *J. Engrg. Mech., ASCE 117*(8), 1865–1877.

Der Kiureghian, A. (1981). Seismic risk analysis of structural systems. *J. Engrg. Mech., ASCE 107*, 1122–1153.

Der Kiureghian, A. and J. B. Ken (1988). The stochastic finite element method in structural reliability. *Probabilistic Engineering Mechanics 3*(2), 83–91.

Der Kiureghian, A., H. Z. Lin, and S. J. Hwang (1987). Second-order reliability approximations. *J. Engrg. Mech., ASCE 113*(8), 1208–1225.

Dym, C. L. and R. E. Levitt (1991). *Knowledge-Based Systems in Engineering.* McGraw-Hill Book Co., Inc.

Faravelli, L. (1989). A response surface approach for reliability analysis. *J. Engrg. Mech., ASCE 115*(2), 2763–2781.

Frangopol, D. M. (1985). Multicriteria reliability-based optimum design. *Structural Safety 3*(1), 23–28.

French, S. (1988). *Decision Theory: An Introduction to the Mathematics of Rationality.* Wiley and Sons.

Fu, G. and D. M. Frangopol (1990a). Balancing weight, system reliability and redundancy in a multiobjective optimization framework. *Structural Safety* (7), 165–175.

Fu, G. and D. M. Frangopol (1990b). Reliability-based vector optimization of structural systems. *J. Engrg. Mech., ASCE 116*(8), 2141–2161.

Gutenberg, B. and C. Richter (1958). Earthquake magnitude, intensity and acceleration. *Bull. Seism. Soc. Am. 62*(2), 105–145.

ICBO (1994). *Uniform Building Code.* International Conference of Building Officials.

Igusa, T. and A. Der Kiureghian (1988). Response of uncertain systems to stochastic excitation. *J. Engrg. Mech., ASCE 114*(5), 812–832.

Katafygiotis, L. S. and C. Papadimitriou (1996). Dynamic response variability of structures with uncertain properties. *Earthquake Engineering and Structural Dynamics 25*(8), 775–793.

Keeney, R. L. and H. Raiffa (1976). *Decisions with Multiple Objectives: Preferences and Value Trade-offs.* Wiley and Sons.

Lin, Y. K. (1967). *Probabilistic Theory of Structural Dynamics.* McGraw Hill.

Lutes, L. D. and S. Sarkani (1997). *Stochastic Analysis of Structural and Mechanical Vibrations.* Prentice-Hall, Inc.

Madsen, H. O., S. Krenk, and N. C. Lind (1986). *Methods of Structural Safety.* Prentice-Hall, Inc.

Masri, S., G. Bekey, and F. Safford (1980). An adaptive random search method for identification of large scale nonlinear systems. *App. Math. and Computation 7*, 353–375.

May, B. S. and J. L. Beck (1998). Probabilistic control for the active mass driver benchmark structural model. *Journal of Earthquake Engineering and Structural Dynamics.*

Moses, F. and D. E. Kisner (1967). Optimal structural design with failure probability constraints. *AIAA Journal 5*(6), 1152–1158.

Otto, K. (1992). *A Formal Representation Theory for Engineering Design.* Ph. D. thesis, California Institute of Technology.

Papadimitriou, C., J. L. Beck, and L. S. Katafygiotis (1995). Asymptotic expansions for reliabilities and moments of uncertain dynamic systems. Technical Report EERL95-05, California Institute of Technology, Pasadena, CA.

Papadimitriou, C., J. L. Beck, and L. S. Katafygiotis (1997). Asymptotic expansions for reliabilities and moments of uncertain dynamic systems. *J. Engrg. Mech., ASCE 123*(12), 1219–1229.

Papadimitriou, C., L. S. Katafygiotis, and S. K. Au (1997). Effects of structural uncertainties on TMD design: A reliability-based approach. *Journal of Structural Control 4*(1), 65–88.

Polidori, D. C., J. L. Beck, and C. Papadimitriou (1998). New approximations for reliability integrals. *J. Engrg. Mech., ASCE*. accepted for publication.

Press, W. H., B. P. Flannery, S. A. Teukolsky, and W. Vetterling (1986). *Numerical Recipes.* Cambridge University Press.

Schuëller, G. I. and R. Stix (1987). A critical appraisal of methods to determine failure probabilities. *Structural Safety 4*, 293–309.

SEAOC (1995). Vision 2000: Performance based seismic engineering of buildings. Technical Report Vol. 1, Part 1, Chap. 2, Structural Engineers Association of California, CA, USA.

Spanos, P. D. and R. Ghanem (1989). Stochastic finite element expansion for random media. *J. Engrg. Mech., ASCE 115*(5), 1035–1053.

Thoft-Christensen, P. and Y. Murotsu (1986). *Application of Structural Systems Reliability Theory.* Springer-Verlag.

Wen, Y. K. (1995). Building reliability and code reliability. *Earthquake Spectra 11*(2), 269–296.

Yang, C.-M. and J. L. Beck (1998). Generalized trajectory methods for finding multiple extrema and roots of functions. *Journal of Optimization Theory and Applications 97*(1), 211–227.